

Design, Synthesis, and Biological Evaluation of Potent c-Met Inhibitors

Noel D. D'Angelo,^{*,†} Steven F. Bellon,[‡] Shon K. Booker,[†] Yuan Cheng,[†] Angela Coxon,[§] Celia Dominguez,[†] Ingrid Fellows,[†] Douglas Hoffman,^{||} Randall Hungate,[†] Paula Kaplan-Lefko,[§] Matthew R. Lee,[‡] Chun Li,[⊥] Longbin Liu,[†] Elizabeth Rainbeau,[†] Paul J. Reider,[†] Karen Rex,[§] Aaron Siegmund,[†] Yaxiong Sun,[‡] Andrew S. Tasker,[†] Ning Xi,[†] Shimin Xu,[†] Yajing Yang,[§] Yihong Zhang,[§] Teresa L. Burgess,[§] Isabelle Dussault,[§] and Tae-Seong Kim[†]

Departments of Medicinal Chemistry, Molecular Structure, Oncology Research, Pharmaceuticals, and Pharmacokinetics and Drug Metabolism, Amgen Inc., One Amgen Center Drive, Thousand Oaks, California 91320-1799

Received May 23, 2008

c-Met is a receptor tyrosine kinase that plays a key role in several cellular processes but has also been found to be overexpressed and mutated in different human cancers. Consequently, targeting this enzyme has become an area of intense research in drug discovery. Our studies began with the design and synthesis of novel pyrimidone **7**, which was found to be a potent c-Met inhibitor. Subsequent SAR studies identified **22** as a more potent analog, whereas an X-ray crystal structure of **7** bound to c-Met revealed an unexpected binding conformation. This latter finding led to the development of a new series that featured compounds that were more potent both in vitro and in vivo than **22** and also exhibited different binding conformations to c-Met. Novel c-Met inhibitors have been designed, developed, and found to be potent in vitro and in vivo.

Introduction

c-Met is a receptor tyrosine kinase that is normally activated by binding its natural ligand hepatocyte growth factor, also known as scatter factor (HGF/SF^a). The binding of HGF to c-Met induces several complex signaling pathways and results in cell proliferation, motility, migration, and survival.^{1–3} These cellular activities are important during normal development and wound healing but can lead to cancer when the pathway is deregulated. For example, c-Met has been found to be overexpressed or mutated in human cancers, and in many instances, the overexpression of c-Met has been correlated with advanced disease stage and poor prognosis.^{4–7} As a result, c-Met has attracted considerable attention as a potential target for cancer treatment.^{8–10}

A variety of approaches have been used to target c-Met. These include antibody-based therapies,^{11–14} truncated HGF fragments,^{15–17} decoy receptors,¹⁸ the targeting of the extracellular c-Met semaphorin domain to prevent dimerization,¹⁹ ribozyme-based treatments,^{20,21} and small-molecule kinase inhibitors.^{22–28} Most of the strategies prevent ligand-mediated activation of the receptor, but small-molecule inhibitors are predicted to inhibit c-Met activity irrespective of the activation mechanism. This

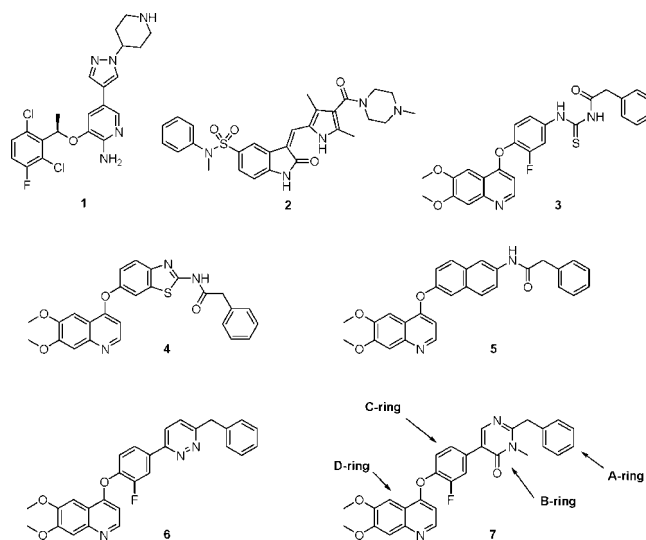


Figure 1. Small-molecule c-Met inhibitors and the design of the pyrimidone series.

is significant because it is known that c-Met can be activated in a ligand-dependent manner as well as in a ligand-independent manner.⁶ Therefore, a small-molecule c-Met inhibitor could benefit a different, and potentially larger, cancer patient population.

Several small-molecule c-Met inhibitors have recently been reported.²⁵ Examples of these include Pfizer's PF-2341066 (**1**),²⁶ Sugen's SU11274 (**2**),²³ and Kirin's acylthiourea **3**²⁹ (Figure 1). Compound **3** was of particular interest because of its reported cellular activity (IC₅₀ = 8.7 nM in A431 cells). This led us to consider constrained versions of **3** as possible c-Met inhibitors. We first examined benzothiazole **4** and found it to be a potent c-Met inhibitor (c-Met K_i = 17 nM). However, its selectivity over other kinases such as kinase insert domain receptor (KDR), recepteur d'origine nantais (RON), and insulin-like growth factor receptor (IGFR) was modest (4- to 13-fold).³⁰ Our replacing the benzothiazole core with a naphthalene ring system (**5**) decreased c-Met potency

* To whom correspondence should be addressed. Address: One Amgen Center Drive, Mail Stop 29-2-C, Thousand Oaks, CA 91320-1799. Phone: 805-313-6550. Fax: 805-480-3016. E-mail: dangelo@amgen.com.

[†] Department of Medicinal Chemistry.

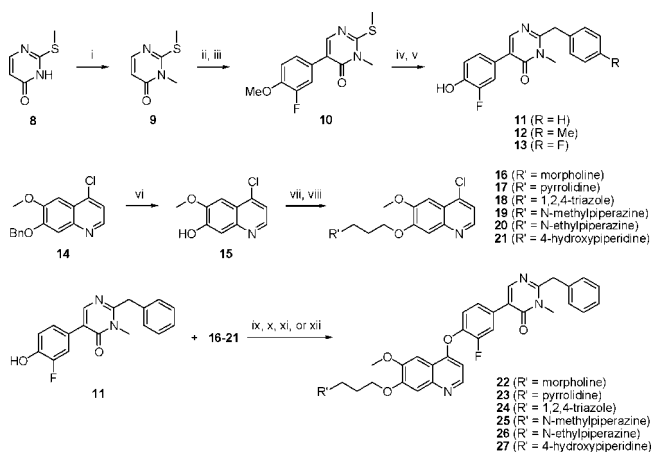
[‡] Department of Molecular Structure.

[§] Department of Oncology Research.

^{||} Department of Pharmaceuticals.

[⊥] Department of Pharmacokinetics and Drug Metabolism.

^a Abbreviations: Ac, acetyl; ANOVA, analysis of variance; ATP, adenosine triphosphate; BSA, bovine serum albumin; DCM, dichloromethane; DMAP, 4-dimethylaminopyridine; DME, 1,2-dimethoxyethane; DMF, *N,N*-dimethylformamide; ED, effective dose; HGF, hepatocyte growth factor; HTRF, homogeneous time-resolved fluorescence; IGFR, insulin-like growth factor receptor; IP, intraperitoneal injection; iv, intravenous; KDR, kinase insert domain receptor; LiHMDS, lithium hexamethyldisilazide; NBS, *N*-bromosuccinimide; PD, pharmacodynamic; PK, pharmacokinetic; RON, recepteur d'origine nantais; SAR, structure–activity relationship; SF, scatter factor; S-Phos, 2-Dicyclohexylphosphino-2',6'-dimethoxybiphenyl; TFAA, trifluoroacetic anhydride; TFA, trifluoroacetic acid; THF, tetrahydrofuran.

Scheme 1^a

^a Reagents and conditions: (i) LiHMDS, DMF, MeI, 0 °C to rt; (ii) Br₂, CHCl₃, 0 °C; (iii) 3-fluoro-4-methoxyphenylboronic acid, Pd₂(dba)₃, S-Phos, K₃PO₄, PhMe, 100 °C; (iv) ArylZnCl, Pd(PPh₃)₄, THF, 60 °C; (v) HOAc, HBr, 120 °C; (vi) MeSO₃H, TFA, reflux; (vii) Cl(CH₂)₃Br, K₂CO₃, DMF; (viii) amine, NaI, K₂CO₃, DMF, 70 °C; (ix) DMAP, 1,4-dioxane, 110 °C; (x) pyridine, 1,4-dioxane, 110 °C; (xi) DMAP, 1,4-dioxane, 120 °C, μ W; and (xii) DMAP, pyridine, 1,4-dioxane, 90 °C, μ W.

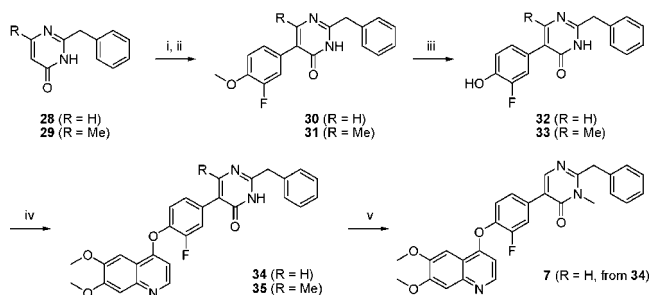
(K_i = 89 nM) but had little effect on KDR and RON selectivity (9- and 3-fold, respectively). Greater selectivity, especially against KDR, was desired to limit potential off-target toxicity as well as to ensure that any *in vivo* activity was a consequence of targeting *c*-Met. Nevertheless, we were encouraged by the fact that a conformational restriction of compound **3** could provide potent *c*-Met inhibitors.

Therefore, we considered an alternative mode of constraining the acylthiourea moiety of compound **3**, which led to the design of pyridazine **6** and pyrimidone **7**. The former was actually more potent against KDR (K_i = 56 nM) and RON (K_i = 79 nM) than against *c*-Met (K_i = 201 nM) and was therefore not pursued further. However, **7** was found to inhibit the kinase activity of *c*-Met (K_i = 39 nM) potently. In addition, **7** was selective against KDR (greater than 30-fold), RON (20-fold), and IGFR (50-fold). With this promising result, we explored the SAR around the four main regions of **7** (rings A–D).

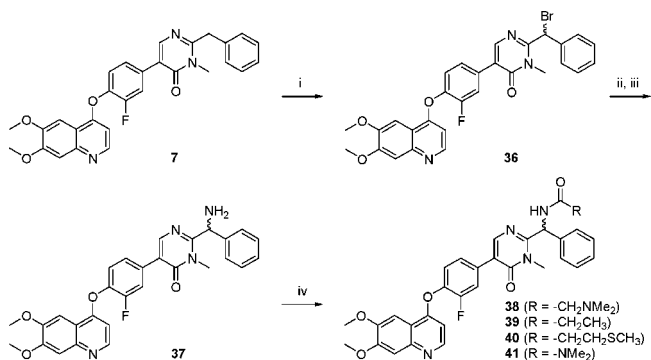
Chemistry

The synthesis of the D-ring analogs began with the alkylation of pyrimidone **8**³¹ at the N(3) position to provide pyrimidone **9** (Scheme 1). Bromination, followed by a Suzuki coupling with 3-fluoro-4-methoxyphenylboronic acid that used the palladium-*S*-Phos complex afforded bicycle **10**.³² O-demethylation, followed by the coupling of the methylthiopyrimidine moiety to various benzylzinc halides, afforded phenols **11**–**13**.³³ Chlorides **16**–**21** were prepared in three routine steps via the debenzoylation of quinoline **14**,³⁴ the attachment of the 3-chloropropyl group, and the displacement of the terminal chloride by the desired amine. Chlorides **16**–**21** were coupled to phenol **11** in the presence of pyridine or DMAP to produce analogs **22**–**27**.

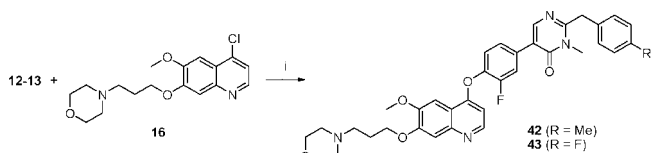
The B-ring analogs were prepared next. Bromination of pyrimidones **28** and **29**,^{35–37} followed by Suzuki coupling to 3-fluoro-4-methoxyphenylboronic acid, afforded methyl ethers **30** and **31** (Scheme 2).³⁸ The removal of the methyl ether under acidic conditions produced phenols **32** and **33**, which were subjected to S_NAr coupling with 4-chloro-6,7-dimethoxyquinoline to afford analogs **34** and **35**. N-methylation of **34** by the use of sodium hydroxide and methyl iodide afforded compound **7**, thereby completing the synthesis of the B-ring set of analogs.

Scheme 2^a

^a Reagents and conditions: (i) Br₂, CHCl₃, 0 °C; (ii) 3-fluoro-4-methoxyphenylboronic acid, Pd(PPh₃)₄, Na₂CO₃, DME, H₂O, 100 °C, μ W; (iii) HOAc, HBr, 120 °C; (iv) 4-chloro-6,7-dimethoxyquinoline, DMAP, PhMe, CHCl₃, 180 °C; and (v) 2 N NaOH, MeI, 1,4-dioxane, 40 °C.

Scheme 3^a

^a Reagents and conditions: (i) NBS, CHCl₃; (ii) NaN₃, DMF, 0 °C; (iii) H₂, Pd/C, EtOAc, THF; and (iv) RCOCl, Et₃N, DCM, 0 °C.

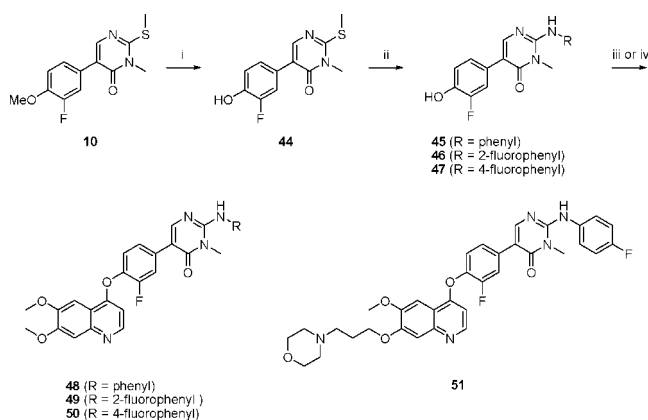
Scheme 4^a

^a Reagents and conditions: (i) Cu, KOH, DMF, pyridine, 110 °C, μ W.

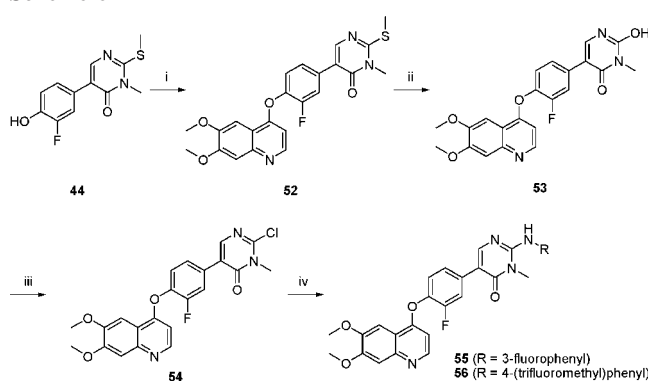
Compound **7** served as a convenient intermediate to prepare analogs that are substituted at the benzylic position. Benzylic bromination converted **7** into bromide **36**, and the subsequent displacement of this bromide with sodium azide, followed by hydrogenation, afforded amine **37** as a racemic mixture (Scheme 3). Acylation of this amine under standard conditions afforded amides **38**–**40** and urea **41**. We prepared two other A-ring analogs by coupling phenols **12** and **13** to chloride **16** to produce compounds **42** and **43**, with a para-methyl and a para-fluoro substituent, respectively (Scheme 4).

The synthesis of the N-linked A-ring analogs began with the demethylation of biaryl **10** to produce phenol **44** (Scheme 5). The displacement of the thiomethyl group under acidic conditions with different anilines in the microwave produced phenols **45**–**47**. The coupling of these phenols to either chloride **16** or 4-chloro-6,7-dimethoxyquinoline produced compounds **48**–**51**.

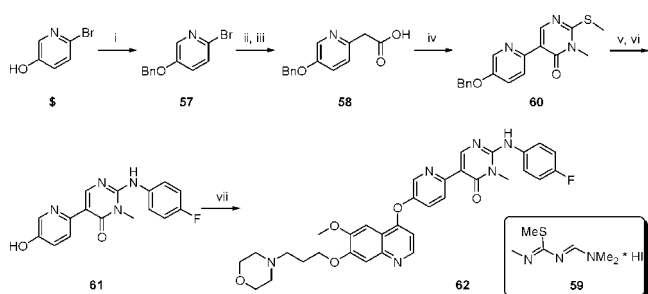
Analog **55** and **56** were prepared in a slightly different manner because phenol **44** was first coupled to 4-chloro-6,7-dimethoxyquinoline to produce intermediate **52** (Scheme 6). The thiomethyl group was hydrolyzed under oxidative conditions by the use of urea hydrogen peroxide in acetonitrile and TFA to produce **53**. The resultant hydroxyl moiety was converted to

Scheme 5^a

^a Reagents and conditions: (i) HOAc, HBr, 120 °C; (ii) RNH₂, concd HCl, 120 °C, μ W; (iii) 4-chloro-6,7-dimethoxyquinoline, DMAP, 1,4-dioxane, 120 °C, μ W; and (iv) **16**, Cu, KOH, DMF, pyridine, 110 °C, μ W.

Scheme 6^a

^a Reagents and conditions: (i) 4-chloro-6,7-dimethoxyquinoline, DMAP, pyridine, 1,4-dioxane, 110 °C; (ii) urea hydrogen peroxide, TFA, MeCN, 0 °C; TFAA, 0 °C to rt; (iii) POCl₃, *N,N*-dimethylaniline, 125 °C to rt; and (iv) RNH₂, concd HCl, 1,4-dioxane, 60 °C, μ W.

Scheme 7^a

^a Reagents and conditions: (i) NaH, BnBr, DMF, 0 °C to rt; (ii) Pd(PPh₃)₄, *t*-BuOC(O)CH₂ZnCl, THF, 60 °C; (iii) TFA, DCM, 0 °C to rt; (iv) (COCl)₂, DCM, DMF; **59**, Et₃N, 0 °C to greater than rt; (v) 4-fluoroaniline, concd HCl, 1,4-dioxane, 125 °C; (vi) BBr₃, DCM; and (vii) **16**, DMAP, pyridine, 1,4-dioxane, 130 °C.

the corresponding chloride **54** by the use of POCl₃. The subsequent displacement of the chloride with different amines, again under acidic conditions in the microwave, produced analogs **55** and **56**.

We prepared C-ring pyridine analog **62** by beginning with the protection of commercially available 6-bromopyridin-3-ol as benzyl ether **57** (Scheme 7). Negishi coupling to 2-*tert*-butoxy-2-oxoethylzinc chloride, followed by TFA hydrolysis, afforded acid **58**.³⁹ The conversion of **58** to the corresponding acyl chloride, followed by the addition of **59** and Et₃N, produced

60. This was converted to phenol **61** in two steps and was then coupled to chloride **16** to afford **62**.

Results and Discussion

SAR and Lead Generation. The enzyme activity of **7** supported our hypothesis that the pyrimidone series could afford good enzyme potency against *c*-Met. To facilitate subsequent SAR studies, we examined the X-ray structure of a cocrystal of **7** bound to *c*-Met (Figure 2). This X-ray revealed that **7** occupies the ATP binding site of *c*-Met. As a result, **7** can be assumed to be an ATP-competitive inhibitor of *c*-Met. In addition, the benzyl moiety of **7** (ring A) fits into a hydrophobic pocket that is formed by ILE1145 at the back end, which we refer to as the ILE1145 binding pocket. This pocket could be probed with different phenyl substituents to improve potency. Also, the benzyl position is orientated toward a channel in the *c*-Met backbone, which suggests that benzyl substituents could fit into this channel and provide additional interactions with *c*-Met.

In terms of the pyrimidone B ring, the X-ray revealed that the carbonyl is twisted away from the Asp1222 residue and directly forms a hydrogen bond with Lys1110. As a result, the polar Asp1222 residue is presented with the hydrophobic C–H group of the B ring, which suggests a potential energy penalty. In addition, there is a fairly tight steric environment around the B and C rings; therefore, we expected SAR opportunities here to be more limited.

The quinoline portion (ring D) on the left side forms hydrogen bonds with the Pro1158 and Met1160 residues and also maintains van der Waals interactions with the *c*-Met backbone. In addition, this quinoline system is directed toward a solvent-exposed area, which provides an opportunity for the introduction of polar, water-solubilizing groups. We began our optimization studies of **7** here.

The introduction of a carbon tether, which contains different tertiary amines, off of the quinoline D-ring was examined first. A three-carbon tether between these amines and the quinoline had previously been determined to be the optimal length for improving the potency; therefore, we examined different amines at the end of this tether.^{40,41} All of the amines improved the *c*-Met enzyme relative to **7**, a finding that can be explained by the van der Waals interactions that are gained between the carbon tether and the *c*-Met backbone (Table 1). Of these amines, the morpholine (**22**) and *N*-methylpyrazine (**25**) derivatives afforded the greatest increase in potency.

Substitutions of the B-ring pyrimidone core were explored next (Table 2). The removal of the *N*-methyl group (**34**) reduced enzyme potency by about 3-fold, whereas the introduction of a methyl group at the 6-position (**35**) lowered the potency by an additional factor of 5. Overall, these two changes reduced the potency more than 10-fold, which supports the hypothesis that this portion of the molecule is sensitive to substitution. In view of these results, we did not pursue further SAR studies around the pyrimidone core or on the fluorophenyl C ring.

We conducted SAR studies to explore different substituents at the benzyl position and on the phenyl A ring. For the former, the X-ray cocrystal structure of **7** (Figure 2) suggested that substituents could gain van der Waals interactions with a channel in the *c*-Met backbone, thereby improving potency. In addition, because this channel was solvent accessible, polar substituents were considered. However, amine **37**, amides **38–40**, and urea **41** provided little improvement in potency (Table 3). In fact, **41** decreased the potency by about 10-fold. Overall, these results

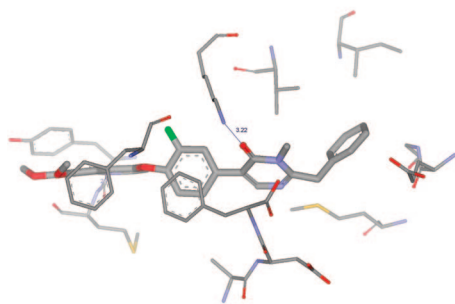
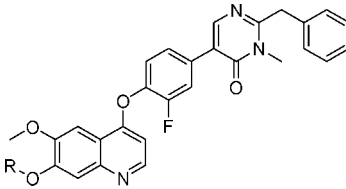
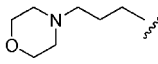
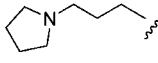
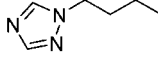
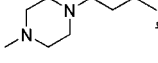
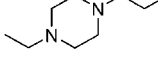
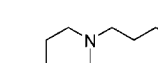


Figure 2. X-ray cocrystal of **7** bound to *c*-Met.

Table 1. *c*-Met Enzyme Activity of Analogs **22**–**27**^a



compd	R	K _i (nM) ^b
7	Me	39 ± 6
22		8.9 ± 1.3
23		12 ± 1
24		29 ± 2
25		9.2 ± 1.4
26		21 ± 1
27		33 ± 6

^a See the Experimental Section for assay details. ^b Average of four experiments.

suggested that whereas the benzyl substitution could certainly be tolerated, no obvious benefit was gained from it.

In terms of the phenyl ring SAR, two additional analogs were made that incorporated different substituents at the para position (Table 4). These compounds had enzyme potencies that were similar to that of **22**, which suggests that small substituents were well tolerated at this position. Because these compounds had enzyme potencies that were similar to that of **22** and also because SAR studies on the nitrogen-linked A rings (see Table 5) indicated that these substituents provided the best increase in potency, further SAR studies were not pursued.

N-Phenyl Analogs. To this point, the most potent compounds exhibited a K_i of around 10 nM in the enzyme assay. However,

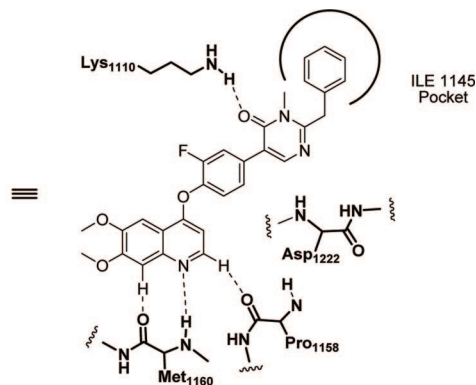
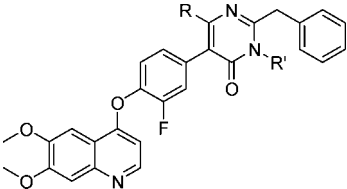


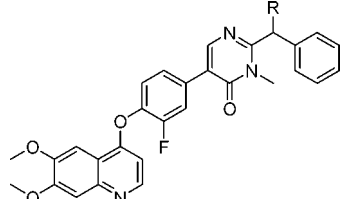
Table 2. *c*-Met Enzyme Activity of B-Ring Analogs **7**, **34**, and **35**^a



compd	R	R'	K _i (nM) ^b
7	H	Me	39 ± 6
34	H	H	107 ± 4
35	Me	H	489 ± 74

^a See the Experimental Section for assay details. ^b Average of four experiments.

Table 3. *c*-Met Enzyme Activity of Benzyl-Substituted A-Ring Analogs^a



compd	R	K _i (nM) ^b
7	H	39 ± 6
37	NH ₂	72 ± 11
38	NH(CO)CH ₂ NMe ₂	30 ± 5
39	NH(CO)CH ₂ CH ₃	71 ± 14
40	NH(CO)CH ₂ CH ₂ SCH ₃	52 ± 11
41	NH(CO)NMe ₂	368 ± 55

^a See the Experimental Section for assay details. ^b Average of four experiments.

to improve the potency further, we next considered replacing the carbon linkage between the A and B rings with a nitrogen atom. This change would allow for an additional hydrogen bond to be gained with Phe1223 (adjacent to Asp1222, Figure 2), potentially via a bridging water molecule, thereby improving enzyme potency.

To test this hypothesis, *N*-phenyl analog **48** was synthesized, and the SAR around the phenyl A ring was explored (Table 5). Our replacing the carbon linkage with a nitrogen linkage actually reduced the enzyme potency to a small extent, as a comparison of compounds **7** and **48** indicates. The introduction of a fluoro group at the ortho or meta position had a minimal impact on enzyme potency. However, substitution at the para position increased the potency because the 4-fluoro derivative (**50**) has a binding affinity of 14 nM. Larger groups at this position (e.g.,

Table 4. c-Met Enzyme Activity of A-Ring Analogs **42** and **43**^a

compd	R	K_i (nM) ^b
22	H	8.9 ± 1.3
42	Me	9.6 ± 0.7
43	F	17 ± 2

^a See the Experimental Section for assay details. ^b Average of four experiments.

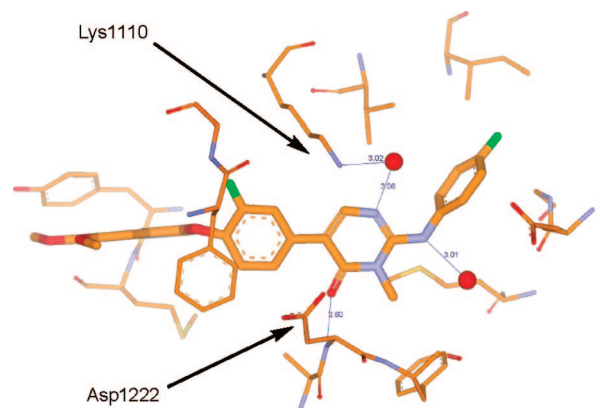
Table 5. c-Met Enzyme Activity of *N*-Phenyl A-Ring Analogs^a

compd	R'	R	K_i (nM) ^b
48	Me	H	63 ± 7
49	Me	2-F	45 ± 4
50	Me	4-F	14 ± 1
51		4-F	4.9 ± 0.5
55	Me	3-F	38 ± 6
56	Me	4-CF ₃	136 ± 12

^a See the Experimental Section for assay details. ^b Average of four experiments.

56) decreased the potency, which suggests that the substitution at this position is fairly sensitive to a substituent's steric size. Having determined that the 4-fluoro group provided the best potency for the *N*-phenyl A ring we decided to reintroduce the morpholine tail off of the quinoline D ring to improve the potency further. Toward this end, analog **51** was prepared and was found to be about 3 times more potent than both **50** and carbon-linked analog **43**, which indicates that our changing the carbon linkage to a nitrogen linkage has a beneficial impact on enzyme activity.

An X-ray cocrystal structure of **50** provided some insight into this observation (Figure 3). Surprisingly, the binding conformation of **50** differed significantly from that of **7**. Most notably, the pyrimidone carbonyl of **50** forms a direct hydrogen bond with the backbone of Asp1222, whereas C-linked analog **7** has its carbonyl pointed toward the Lys1110 primary amine (Figure 2). In addition, the N(1) pyrimidone nitrogen of **50** is bridged to Lys1110 through hydrogen bonding to a crystallographically resolved water molecule, which indirectly preserves the hydrogen bond between the pyrimidone carbonyl of **7** and this amino acid. Therefore, the different pyrimidone orientation results in

**Figure 3.** X-ray cocrystal of **50** bound to c-Met.

the formation of an additional hydrogen bond with c-Met. A comparison of Figures 2 and 3 reveals that the A and C rings of both compounds adopt the same orientation relative to the c-Met backbone. Therefore, the conformational preferences of these two compounds dictate their respective pyrimidone B-ring orientations and hence their binding conformations to the protein. The additional hydrogen bond that was gained as a result of the changed pyrimidone conformation and the introduction of the para-fluoro substituent are the most plausible explanations of the increase in potency that was observed with nitrogen-linked compounds (e.g., **50** and **51**) compared with carbon-linked compounds (e.g., **7**). It should be noted that **50**, like **7**, binds to c-Met in the ATP pocket which indicates that **50** is an ATP-competitive inhibitor. This conclusion can also be applied to other pyrimidone molecules such as **22** and **51** because of their structural similarities to **7** and **50**, respectively.

The X-ray cocrystal of **50** also provided another clue as to how enzyme potency could be further improved. The dihedral angle between the fluorophenyl C ring and the pyrimidone B ring is 18°. To determine whether this dihedral angle corresponds to an energetically favored conformation, we examined an energy diagram that used 5-phenylpyrimidone as a surrogate for the B and C rings (Figure 4, top). As this graph indicates, a dihedral angle of 18° is about 1.5 kcal/mol above the energy minimum, which suggests that compounds like **50** and **51** incur a significant energy penalty to adopt the conformation with which they bind to c-Met.

To eliminate this energy barrier, we envisioned replacing the fluorophenyl C ring with a pyridine ring on the basis of the energy diagram of pyridin-2-yl pyrimidone (Figure 4, bottom). This diagram suggests that for a pyridine ring a dihedral angle of 20° or less provides the lowest energy conformation, which is in contrast with the phenylpyrimidone systems in which such a dihedral angle is energetically disfavored. As a result, we expected analogs with a pyridine B ring to be more potent because of the low-energy barrier that is required for them to bind c-Met. On the basis of this reasoning, we examined analog **62** and found it to be one of the most potent analogs of the series thus far ($K_i = 3.4 \pm 0.7$ nM). However, the increase in potency compared with that of **51** ($K_i = 4.9$ nM) was virtually negligible, at least in the enzyme assay. This could be the result of removing the C-ring fluoro group, a change that could offset any gain in potency that was obtained by the use of the pyridine ring.

In Vitro Cell Assays. Some of the more potent compounds that were identified in the enzyme assay were tested for their ability to inhibit HGF-mediated c-Met phosphorylation in PC3 cells, a human prostate cancer cell line, and CT26 cells, a murine

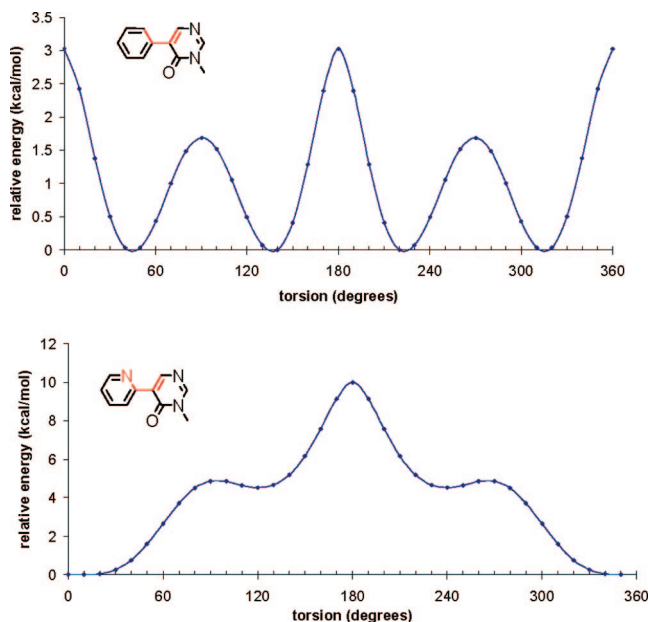


Figure 4. Torsional profiles of 5-phenyl pyrimidone (top) and pyridin-2-yl pyrimidone (bottom) for the dihedral angle highlighted in red. The coplanar structures shown are defined with a dihedral angle of 0°. Energy profiles were calculated on the basis of gas-phase quantum mechanic calculations by the use of density functional theory.

Table 6. IC₅₀ Values of Lead Analogs Against PC3 and CT26 Cell Lines^a

compd	K _i (nM) ^b	PC3 IC ₅₀ (nM) ^b	CT26 IC ₅₀ (nM) ^b
7	39	313	368
43	17	161	196
51	4.9	64	82
62	3.4	39	59

^a See the Experimental Section for assay details. ^b Average of four experiments, with the exception of the PC3 and CT26 values for **62**, which are the average of two experiments.

cell line that is derived from a colon carcinoma (Table 6). In general, the compounds were slightly more potent in PC3 cells than they were in CT26 cells. In addition, the compounds generally exhibited a 10-fold shift in potency from enzyme to cell. Most significantly, the trends observed for enzyme potency for these compounds correlated with those that were observed for their cellular activities. Thus, the conversion of **7** to **43** resulted in improved cell potency as well as improved enzyme potency. Our changing the carbon linkage of **43** to a nitrogen linkage (**51**) improved enzyme and cellular potencies by an additional factor of 3. Finally, our replacing the fluorophenyl C ring of **51** with a pyridine ring (**62**) further improved cellular potency and made **62** the most potent analog that was prepared in this series.

Enzyme Selectivity. The selectivity of certain compounds against KDR, RON, and IGFR was examined next, and the results are outlined in Table 7. A noticeable trend is that the carbon-linked compounds (**7**, **22**, and **43**) were more selective against these enzymes than were the nitrogen-linked compounds (**50**, **51**, and **62**). This result might be explained by the differences in binding conformations that are demonstrated by **7** (Figure 2) and **50** (Figure 3). In particular, the different selectivity profiles most likely are the result of the different pyrimidone orientations because the A and C rings virtually occupy the same space in both cases. Whereas the decrease in selectivity was undesirable, the selectivity, especially that against KDR, was still high enough for **51** and **62** to justify further in vivo studies on these compounds, as well as on **22**.

Table 7. Enzyme Selectivity of Key Compounds^a

compd	c-Met K _i (nM) ^b	KDR K _i (nM) ^{c,d}	Ron K _i (nM) ^{e,f}	IGFR K _i (nM) ^f
7	39	>1300	581	1030
22	8.9	422	195	1450
43	17	>3000	706	860
50	14	382	80	70
51	4.9	139	28	22
62	3.4	83	1.3	51

^a See the Experimental Section for assay details. ^b Average of four experiments. ^c Value is the result of a single measurement, with the exception of **22**, which is the average of two experiments. ^d Phosphorylated KDR. ^e Phosphorylated Ron. ^f Value is the result of a single experiment.

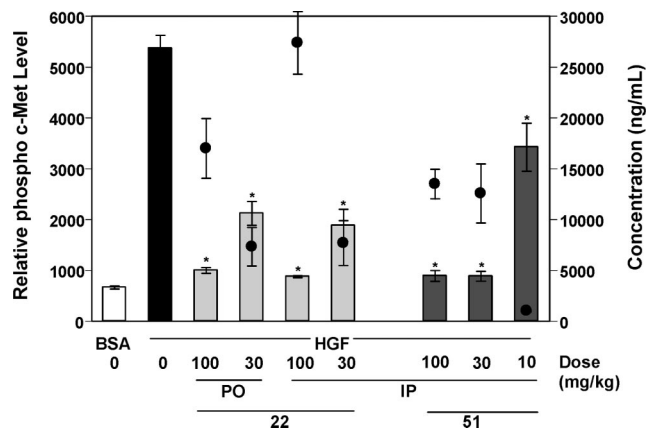


Figure 5. Effect of **22** and **51** on HGF-mediated c-Met phosphorylation at 2 h postdose. Asterisk denotes $p < 0.0001$ compared with the HGF group (black bar). Bars represent the mean \pm standard deviation ($n = 3$). Circles represent mean plasma concentration \pm standard deviation.

The selectivities of compounds **22**, **51**, and **62** were also examined against a larger panel of tyrosine kinases and serine/threonine kinases. In this panel, the three compounds exhibited low selectivity (less than 10-fold) against only a small number of kinases (LCK, BTK, and cFMS). For most of the other examined kinases, selectivities were greater than 100-fold.⁴²

In Vivo Studies. Compound **22** from the carbon-linked series and compounds **51** and **62** from the nitrogen-linked series were evaluated for their pharmacokinetic (PK) properties and pharmacodynamic (PD) effects. All three compounds exhibited good PK profiles when they were given intravenously (iv) to rats, with half lives that ranged from 2.4 to 4 h, volumes of distribution that ranged from 3.0 to 5.4 L/kg, and clearances that ranged from 0.56 to 1.9 L/h/kg. Compound **22** had the highest bioavailability with a value of 100%, whereas **51** and **62** had values of 34 and 48%, respectively. Given the promising PK profiles of these compounds, we decided to evaluate all three compounds in a PD assay.

These compounds were administered to mice by either oral gavage (PO) or intraperitoneal injection (IP) (10, 30, or 100 mg/kg). Recombinant human HGF was injected iv at 2 h postdose. Livers were then harvested, and c-Met phosphorylation was quantified. Treatment with **22**, **51**, and **62** led to the dose-dependent inhibition of c-Met phosphorylation (Figures 5 and 6). Compound **22** exhibited an ED₉₀ of approximately 100 mg/kg (Figure 5). Consistent with the enzyme and cell data, analogs **51** and **62** exhibited increased potencies, with ED₉₀ values of ~30 mg/kg (Figures 5 and 6).

Conclusions

Overall, we have developed a novel and potent chemical series for targeting c-Met in vitro and in vivo. Our initial lead

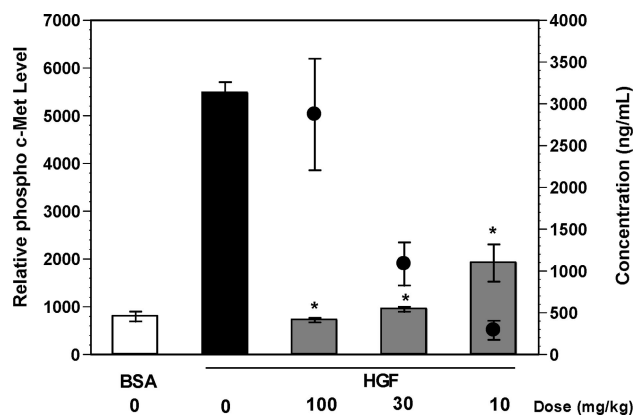


Figure 6. Effect of **62** on HGF-mediated c-Met phosphorylation at 2 h postdose. Asterisk denotes $p < 0.0001$ compared with the HGF group (black bar). Bars represent the mean \pm standard deviation ($n = 3$). Circles represent mean plasma concentration \pm standard deviation.

compound **7** was found to be a potent c-Met inhibitor and was subsequently developed into the more potent analog **22**. However, an X-ray crystal structure of **7** bound to c-Met revealed an unexpected binding conformation. This result led to the design and synthesis of nitrogen-linked A-ring analogs **50** and **51**, which were more potent than **22** both in vitro and in vivo but were also less selective against other enzymes. The X-ray crystal structure of **50** revealed a binding conformation that was different from that of the carbon-linked analogs. This finding helps explain the potency and enzyme selectivity differences between the two series. This X-ray structure led to the design and synthesis of pyridine analog **62** as a means of minimizing dihedral angle strain between the B and C rings. As a result, **62** proved to be the most potent compound in this series both in vitro and in vivo.

Experimental Section

Chemistry. All reactions were conducted on the benchtop and were run under nitrogen by the use of a Teflon-coated magnetic stir bar at the indicated temperature. Reactions that were run at an elevated temperature were run in an oil bath at the indicated temperature. Microwave reactions were run in a CEM Discover microwave that was equipped with the PowerMAX feature that used the settings described below. All solvents and reagents that were obtained from commercial sources were used without further purification. The removal of solvents was conducted by the use of a rotary evaporator, and the residual solvent was removed from nonvolatile compounds by the use of a vacuum manifold that was maintained at ~ 1 torr. All reported yields are isolated yields.

Analytical TLC was performed with EMD 0.25 mm silica gel 60 plates with a 254 nm fluorescent indicator. Plates were developed in a covered chamber and were visualized with ultraviolet light. Flash chromatography refers to column chromatography, as described by Still, that uses EMD silica gel 60 (230–400 mesh) as the stationary phase.⁴³ ISCO purification refers to a Teledyne ISCO purification system that uses RediSep columns in the size that is noted as well as the solvent system and gradients that are noted.

¹H NMR spectra were obtained on a Bruker BioSpin GmbH magnetic resonance spectrometer. ¹H NMR spectra are reported as chemical shifts in parts per million (ppm) relative to an internal solvent reference. Peak multiplicity abbreviations are as follows: s (singlet), br s (broad singlet), d (doublet), dd (doublet of doublets), t (triplet), q (quartet), qn (quintet), and m (multiplet).

We conducted analytical HPLC and mass spectroscopy by the use of a reverse-phase Agilent 1100 series HPLC–MS by using the methods that are noted for each compound in the Supporting Information. The retention time (t_R) was recorded in minutes by

the use of UV detection at 254 nm. High-resolution MS measurements were obtained by the use of electrospray ionization on a Thermo Scientific linear ion trap (LTQ) Orbitrap spectrometer.

Elemental Analyses (C, H, N) were obtained from Atlantic Microlab in Norcross, Georgia.

3-Methyl-2-(methylthio)pyrimidin-4(3H)-one (9). Compound **8** (6.29 g, 44.2 mmol) was suspended in DMF (100 mL) and was cooled to 0 °C, and additional DMF (50 mL) was added. Solid LiHMDS (9.58 g, 57.3 mmol) was added in one portion, and the reaction was stirred at 0 °C. MeI (3.6 mL, 57.8 mmol) was added via syringe, and the reaction was warmed to room temperature and was stirred for 20.75 h. At this time, it was poured into 300 mL of H₂O and was extracted exhaustively with EtOAc. The organic extracts were combined, were dried over Na₂SO₄, were filtered, were concentrated, and were purified on silica gel (3:1 \rightarrow 3:2 \rightarrow 1:1 hexanes/EtOAc) to produce **9** (3.79 g, 55%). ¹H NMR (400 MHz, CDCl₃, δ): 7.76 (d, $J = 6.4$ Hz, 1H), 6.20 (d, $J = 6.4$ Hz, 1H), 3.52 (s, 3H), 2.58 (s, 3H). MS (ES) m/z : 157 (M + H⁺).

5-(3-Fluoro-4-methoxyphenyl)-3-methyl-2-(methylthio)pyrimidin-4(3H)-one (10). Compound **9** (3.31 g, 21.2 mmol) was dissolved in chloroform (50 mL) and was cooled to 0 °C under argon. Bromine (1.25 mL, 25.4 mmol) was added via syringe, and the reaction was stirred at 0 °C for 35 min, at which time TLC analysis indicated the complete consumption of starting material. The reaction was quenched with 40 mL of saturated NaHCO₃, was warmed to room temperature, and was stirred overnight. The reaction was extracted with DCM (3 \times 25 mL), and the organic extracts were combined, were dried over Na₂SO₄, were filtered, and were concentrated to produce 5-bromo-3-methyl-2-(methylthio)pyrimidin-4(3H)-one (4.98 g, 100%), which did not require further purification. ¹H NMR (400 MHz, CDCl₃, δ): 8.07 (s, 1H), 3.58 (s, 3H), 2.58 (s, 3H). MS (ES) m/z : 235 (Br79, M + H⁺), 237 (Br81, M + H⁺).

5-Bromo-3-methyl-2-(methylthio)pyrimidin-4(3H)-one (14.77 g, 62.8 mmol), 3-fluoro-4-methoxyphenylboronic acid (20.11 g, 118.3 mmol), Pd₂(dba)₃ (1.869 g, 2.04 mmol), *S*-Phos (3.45 g, 8.40 mmol), and K₃PO₄ (42.27 g, 199.1 mmol) were suspended in PhMe (200 mL). Argon was bubbled through the solution for 5 min, and the reaction was then placed in a preheated oil bath (100 °C) and was stirred for 6.25 h, at which time LCMS analysis indicated a complete reaction. The reaction was cooled to room temperature and was allowed to stand overnight. It was then diluted with DCM (200 mL) and was filtered through a 1 in plug of silica gel that was washed exhaustively with MeOH, EtOAc, and DCM. (Some solid material that was stuck in the flask had to be taken up in water and extracted with EtOAc separately). The filtrate (and EtOAc extracts) were combined and concentrated, which resulted in an orange solid. This was treated with hexanes and was filtered, and the resultant light-yellow solid was repeatedly washed with hexanes and was dried under high vacuum to afford **10** (15.85 g, 90%) as a light-yellow solid. For analytical purposes, a sample was washed with EtOAc, and the resultant white solid was dried under vacuum. ¹H NMR (400 MHz, CDCl₃, δ): 7.93 (s, 1H), 7.46 (d, $J = 12.8$ Hz, 1H), 7.40 (d, $J = 8.8$ Hz, 1H), 6.99 (t, $J = 8.8$ Hz, 1H), 3.94 (s, 3H), 3.59 (s, 3H), 2.61 (s, 3H). MS (ES) m/z : 281 (M + H⁺).

General Procedure for the Synthesis of 11–13. 2-Benzyl-5-(3-fluoro-4-hydroxy-phenyl)-3-methylpyrimidin-4(3H)-one (11). To a 500 mL three-necked round-bottomed flask that contained **10** (10 g, 36 mmol) and Pd(PPh₃)₄ (4.5 g, 3.9 mmol) in THF (50 mL) was added benzylzinc bromide (100 mL, 0.5 M in THF, 42 mmol). The flask was then placed in a preheated (60 °C) oil bath, and the reaction was stirred for 2 h and was then allowed to cool to ambient temperature. The reaction was quenched with saturated NH₄Cl, DCM (300 mL) was added, and the mixture was stirred overnight. The layers were separated, and the organic phase was collected, was dried over Na₂SO₄, was filtered, and was concentrated.

The crude material was put in a 1000 mL three-necked round-bottomed flask, and acetic acid (140 mL, 31 mmol) and hydrobromic acid (340 mL, 48%, 31 mmol) were added. The flask was fit with a reflux condenser, and the mixture was stirred at 135 °C for 4 h. The mixture was filtered while it was still hot, and the filtrate

was cooled to ambient temperature. The filtrate was filtered, and the solid that was collected was washed with hexanes to afford **11** (9.2 g, 82% over two steps) as an off-white solid. ^1H NMR (400 MHz, CDCl_3 , δ): 8.05 (s, 1H), 7.52 (dd, $J = 12.1, 2.0$ Hz, 1H), 7.40–7.21 (m, 6H), 7.00 (t, $J = 8.8$ Hz, 1H), 6.20 (br s, 1H), 4.20 (s, 2H), 3.51 (s, 3H). MS (ES) m/z : 311 ($\text{M} + \text{H}^+$).

4-Chloro-6-methoxyquinolin-7-ol (15). 7-(Benzyloxy)-4-chloro-6-methoxyquinoline (36 g, 0.11 mol) was dissolved in TFA (200 mL), and $\text{CH}_3\text{SO}_3\text{H}$ (13.9 mL, 0.214 mol) was added in one portion. The reaction was heated at reflux for 3 h and was then cooled to room temperature and concentrated. Aqueous 2.5 N NaOH was added to raise the pH of the solution to 7, which caused precipitation. The resultant solid was crushed, was stirred vigorously for 1 h, and was then filtered. The solid was collected and was dried under high vacuum to afford **15** (22 g, ~100%) as a brown solid. ^1H NMR (400 MHz, d_6 -DMSO, δ): 8.66 (d, $J = 5.0$ Hz, 1H), 7.64 (d, $J = 5.0$ Hz, 1H), 7.42 (s, 1H), 7.40 (s, 1H), 4.00 (s, 3H), 2.31 (s, 1H). MS (ES) m/z : 210 ($\text{M} + \text{H}^+$).

General Procedure for the Synthesis of 16–21. 4-Chloro-6-methoxy-7-(3-morpholino-propoxy)quinoline (16). Compound **15** (11 g, 53 mmol), 3-chloro-1-bromopropane (26 mL, 265 mmol), and K_2CO_3 (69 g, 500 mmol) were suspended in DMF (400 mL) and were stirred at room temperature for 16 h. The suspension was filtered, and the filtrate was concentrated and diluted with EtOAc and water. The organic layer was separated, was dried over Na_2SO_4 , was filtered, and was concentrated to afford a brown solid, which was directly used in the next step.

This brown solid was diluted with DMF (800 mL) and NaI (11.8 g, 79 mmol), and K_2CO_3 (36 g, 265 mmol) and morpholine (27.7 mL, 318 mmol) were added. The reaction was heated to 70 °C and was stirred for 16 h. It was then cooled to room temperature, was diluted with water (2 L), and was extracted two times with EtOAc. The organic extracts were combined, were dried over sodium sulfate, were filtered, and were concentrated to produce a dark-brown solid. This material was recrystallized in DCM–hexanes to afford **16** (12 g, 67% over two steps) as a light-brown solid. ^1H NMR (400 MHz, d_6 -DMSO, δ): 8.60 (d, $J = 4.5$ Hz, 1H), 7.55 (d, $J = 4.5$ Hz, 1H), 7.45 (s, 1H), 7.37 (s, 1H), 4.21 (t, $J = 6.3$ Hz, 2H), 3.97 (s, 3H), 3.60–3.55 (m, 4H), 2.46 (t, $J = 7.0$ Hz, 2H), 2.41–2.35 (m, 4H), 1.97 (qn, $J = 6.0$ Hz, 2H). MS (ES) m/z : 337 ($\text{M} + \text{H}^+$).

General Procedure for the Synthesis of 22–24 and 26. 2-Benzyl-5-(3-fluoro-4-(6-methoxy-7-(3-morpholinopropoxy)quinolin-4-yloxy)phenyl)-3-methylpyrimidin-4(3H)-one (22). Phenol **11** (200 mg, 0.645 mmol), chloride **16** (261 mg, 0.774 mmol), and DMAP (24 mg, 0.20 mmol) were suspended in 1,4-dioxane in a microwave vial. The vial was then sealed and was heated in the microwave to 120 °C at 300 W for 20 min. The reaction was then concentrated and was purified on prep HPLC (1 → 80% MeCN/water with 0.1% TFA over 60 min). The fractions with product were collected, were concentrated, and were diluted with DCM. MP-carbonate beads were added, and the suspension was stirred for 10 min and was filtered. The beads were washed with MeOH and CH_2Cl_2 three times, and the filtrate was concentrated to afford **22** (154 mg, 39%) as a yellow glass. ^1H NMR (400 MHz, CDCl_3 , δ): 8.50 (d, $J = 5.3$ Hz, 1H), 8.15 (s, 1H), 7.72 (dd, $J = 11.6, 2.0$ Hz, 1H), 7.59–7.53 (m, 2H), 7.45 (s, 1H), 7.41–7.25 (m, 6H), 6.49 (dd, $J = 5.3, 0.9$ Hz, 1H), 4.28 (t, $J = 6.7$ Hz, 2H), 4.23 (s, 2H), 4.04 (s, 3H), 3.75–3.70 (m, 4H), 3.55 (s, 3H), 2.58 (t, $J = 7.2$ Hz, 2H), 2.53–2.46 (m, 4H), 2.19–2.08 (m, 2H). MS (ES) m/z : 611 ($\text{M} + \text{H}^+$). Anal. Calcd for $(\text{C}_{35}\text{H}_{35}\text{FN}_4\text{O}_5 \cdot 0.2\text{CH}_2\text{Cl}_2)$: C, H, N.

2-Benzyl-5-(3-fluoro-4-(6-methoxy-7-(3-(pyrrolidin-1-yl)propoxy)quinolin-4-yloxy)-phenyl)-3-methylpyrimidin-4(3H)-one (23). By using chloride **17** and by following the procedure that was used to prepare **22**, we obtained **23** (4%) as a white solid. ^1H NMR (400 MHz, d_6 -DMSO, δ): 8.50 (d, $J = 8.0$ Hz, 1H), 8.30 (s, 1H), 7.93 (dd, $J = 16.0, 4.0$ Hz, 1H), 7.74 (d, $J = 8.0$ Hz, 1H), 7.53 (s, 1H), 7.51 (t, $J = 8.0$ Hz, 1H), 7.41–7.26 (m, 6H), 6.51 (d, $J = 8.0$ Hz, 1H), 4.29 (s, 2H), 4.21 (t, $J = 8.4$ Hz, 2H), 3.96 (s, 3H), 3.52 (s, 3H), 2.62–2.52 (m, 2H), 2.52–2.40 (m, 4H, buried

under DMSO peak), 2.04–1.97 (m, 2H), 1.73–1.65 (m, 4H). MS (ES) m/z : 595 ($\text{M} + \text{H}^+$). HRMS calcd for $\text{C}_{35}\text{H}_{36}\text{FN}_4\text{O}_4$ ($\text{M} + \text{H}^+$), 595.2721; found, 595.2712. Analytical HPLC: 97.9%. $t_R = 5.47$.

5-(4-(7-(3-(1H-1,2,4-Triazol-1-yl)propoxy)-6-methoxyquinolin-4-yloxy)-3-fluorophenyl)-2-benzyl-3-methylpyrimidin-4(3H)-one (24). By using chloride **18**, we prepared compound **24** by following the procedure that was used to prepare **22**, with the following modifications: pyridine (2.5 mL) and 1,4-dioxane (1.25 mL) were both used, and the reaction was run in the microwave at 90 °C and 150 W for 10 min. Compound **24** was isolated in 3% yield as an off-white solid. ^1H NMR (400 MHz, d_6 -DMSO, δ): 8.57 (s, 1H), 8.50 (d, $J = 5.3$ Hz, 1H), 8.29 (s, 1H), 7.99 (s, 1H), 7.92 (dd, $J = 12.5, 1.6$ Hz, 1H), 7.74 (d, $J = 8.3$ Hz, 1H), 7.55 (s, 1H), 7.51 (t, $J = 8.8$ Hz, 1H), 7.41–7.25 (m, 6H), 6.52 (d, $J = 5.3$ Hz, 1H), 4.41 (t, $J = 6.9$ Hz, 2H), 4.28 (s, 2H), 4.18 (t, $J = 6.0$ Hz, 2H), 3.97 (s, 3H), 3.52 (s, 3H), 2.41–2.30 (m, 2H). MS (ES) m/z : 593 ($\text{M} + \text{H}^+$). HRMS calcd for $\text{C}_{33}\text{H}_{30}\text{FN}_6\text{O}_4$ ($\text{M} + \text{H}^+$), 593.2313; found, 593.2299. Analytical HPLC: 96.8%. $t_R = 5.22$.

2-Benzyl-5-(4-(7-(3-(4-ethylpiperazin-1-yl)propoxy)-6-methoxyquinolin-4-yloxy)-3-fluorophenyl)-3-methylpyrimidin-4(3H)-one (26). By using chloride **20**, and by following the procedure that was used to prepare **24**, we obtained **26** (10%) as a white solid. ^1H NMR (400 MHz, d_6 -DMSO, δ): 8.50 (d, $J = 5.1$ Hz, 1H), 8.29 (s, 1H), 7.92 (d, $J = 12.6$ Hz, 1H), 7.74 (d, $J = 8.7$ Hz, 1H), 7.53 (s, 1H), 7.50 (t, $J = 12.0$ Hz, 1H), 7.42–7.25 (m, 6H), 6.51 (d, $J = 4.7$ Hz, 1H), 4.28 (s, 2H), 4.19 (t, $J = 5.8$ Hz, 2H), 3.95 (s, 3H), 3.52 (s, 3H), 2.61–2.30 (m, 12H), 2.05–1.90 (m, 2H), 0.99 (t, $J = 7.0$ Hz, 3H). MS (ES) m/z : 638 ($\text{M} + \text{H}^+$). HRMS calcd for $\text{C}_{37}\text{H}_{41}\text{FN}_5\text{O}_4$ ($\text{M} + \text{H}^+$), 638.3143; found, 638.3135. Analytical HPLC: 97.5%. $t_R = 4.70$.

General Procedure for the Synthesis of 25 and 27. 2-Benzyl-5-(3-fluoro-4-(6-methoxy-7-(3-(4-methylpiperazin-1-yl)propoxy)quinolin-4-yloxy)phenyl)-3-methylpyrimidin-4(3H)-one (25). Phenol **11** (258 mg, 0.832 mmol), chloride **19** (350 mg, 0.999 mmol), and DMAP (10 mg, 0.083 mmol) were suspended in pyridine (4.0 mL) and 1,4-dioxane (1.0 mL) and were heated in an oil bath at 110 °C over the weekend, at which time the solvent evaporated. More pyridine and 1,4-dioxane were added, and stirring was continued until about half of the starting material had been consumed, according to LCMS analysis. The reaction was cooled to room temperature, was concentrated, and was purified on silica gel (0 → 10% 2 M ammonia in MeOH/DCM). The fraction with product was collected, was concentrated, and was purified by HPLC. The fraction with product was treated with ammonium hydroxide and was extracted with 5% MeOH/DCM. The organic extracts were washed with saturated NaHCO_3 , were dried over sodium sulfate, were filtered, and were concentrated to afford **25** (40 mg, 8%) as a light-yellow solid. ^1H NMR (400 MHz, d_6 -DMSO, δ): 8.50 (d, $J = 5.1$ Hz, 1H), 8.29 (s, 1H), 7.92 (dd, $J = 12.5, 2.0$ Hz, 1H), 7.74 (d, $J = 12.0$ Hz, 1H), 7.53 (s, 1H), 7.50 (t, $J = 12.0$ Hz, 1H), 7.41–7.27 (m, 6H), 6.51 (d, $J = 5.3$ Hz, 1H), 4.28 (s, 2H), 4.19 (t, $J = 6.4$ Hz, 2H), 3.95 (s, 3H), 3.52 (s, 3H), 2.46 (t, $J = 7.0$ Hz, 2H), 2.50–2.25 (m, 8H), 2.15 (s, 3H), 1.97 (qn, $J = 10$ Hz, 2H). MS (ES) m/z : 624 ($\text{M} + \text{H}^+$). HRMS calcd for $\text{C}_{36}\text{H}_{39}\text{FN}_5\text{O}_4$ ($\text{M} + \text{H}^+$), 624.2986; found, 624.2962. Analytical HPLC: 98.8%. $t_R = 4.91$.

2-Benzyl-5-(3-fluoro-4-(7-(3-(4-hydroxy-piperidin-1-yl)propoxy)-6-methoxyquinolin-4-yloxy)phenyl)-3-methylpyrimidin-4(3H)-one (27). By using chloride **21**, we prepared compound **27** by following the procedure that was used to prepare **25**, except NMP was used instead of pyridine and was added after the mixture was stirred overnight. Compound **27** was isolated in 6% yield as an off-white solid as a TFA salt. ^1H NMR (500 MHz, CD_3OD , δ): 8.45 (d, $J = 5.5$ Hz, 1H), 8.23 (s, 1H), 7.81 (dd, $J = 11.9, 2.1$ Hz, 1H), 7.67 (s, 1H), 7.65 (d, $J = 7.1$ Hz, 1H), 7.43 (t, $J = 8.4$ Hz, 1H), 7.40–7.36 (m, 3H), 7.33–7.28 (m, 3H), 6.58 (d, $J = 5.2$ Hz, 1H), 4.31 (s, 2H), 4.28 (t, $J = 5.9$ Hz, 2H), 4.03 (s, 3H), 3.77 (br s, 1H), 3.56 (s, 3H), 3.14–3.05 (m, 2H), 2.93–2.86 (m, 2H), 2.65–2.55 (m, 2H), 2.22 (qn, $J = 7.0$ Hz, 2H), 1.99–1.93 (m,

2H), 1.73–1.65 (m, 2H). MS (ES) m/z : 625 (M + H⁺). Analytical HPLC: 98.9%. t_R = 5.32.

General Procedure for the Synthesis of 32 and 33. 2-Benzyl-5-(3-fluoro-4-hydroxy-phenyl)pyrimidin-4(3H)-one (32). We brominated 2-benzyl-pyrimidin-4(3H)-one (**28**) by following the procedure that was used for the bromination of **9** to afford 2-benzyl-5-bromopyrimidin-4(3H)-one in 29% yield.

2-Benzyl-5-bromopyrimidin-4(3H)-one (100 mg, 0.379 mmol), 3-fluoro-4-methoxyphenylboronic acid (128 mg, 0.756 mmol), Pd(PPh₃)₄ (22 mg, 0.019 mmol), and Na₂CO₃ (1 M in water, 0.5 mL, 0.5 mmol) were suspended in DME (1.5 mL) and were heated in the CEM microwave to 100 °C at 75 W for 10 min. The reaction was cooled to room temperature and was diluted with water and DCM. The organic layer was collected, was dried over sodium sulfate, was filtered through celite, and was concentrated. Purification via silica gel chromatography (ISCO column, 12 g, 0 → 5% MeOH/DCM) afforded **30** (86 mg, 74%) as a white solid.

Finally, we converted **30** to phenol **32** by following the demethylation procedure (HBr and HOAc) that was used to prepare **11**. Compound **32** was isolated in 65% yield as a white solid. ¹H NMR (400 MHz, *d*₆-DMSO, δ): 12.88 (s, 1H), 9.98 (s, 1H), 8.09 (s, 1H), 7.58 (dd, J = 13.3, 2.3 Hz, 1H), 7.39–7.30 (m, 5H), 7.29–7.22 (m, 1H), 6.95 (t, J = 8.8 Hz, 1H), 3.89 (s, 2H). MS (ES) m/z : 297 (M + H⁺).

2-Benzyl-5-(3-fluoro-4-hydroxyphenyl)-6-methylpyrimidin-4(3H)-one (33). Compound **33** was prepared from 2-benzyl-6-methyl-pyrimidin-4(3H)-one (**29**) with the same three-step sequence that was used to synthesize **32**. ¹H NMR (400 MHz, *d*₆-DMSO, δ): 12.67 (br s, 1H), 9.90 (br s, 1H), 7.39–7.31 (m, 4H), 7.28–7.23 (m, 1H), 7.03 (dd, J = 12.6, 2.0 Hz, 1H), 6.94 (t, J = 8.8 Hz, 1H), 6.85 (dd, J = 8.4, 1.6 Hz, 1H), 3.83 (s, 2H), 2.07 (s, 3H). MS (ES) m/z : 311 (M + H⁺).

2-Benzyl-5-(4-(6,7-dimethoxyquinolin-4-yloxy)-3-fluorophenyl)pyrimidin-4(3H)-one (34). Compound **32** (100 mg, 0.334 mmol), 4-chloro-6,7-dimethoxyquinoline (113 mg, 0.505 mmol), and DMAP (41 mg, 0.336 mmol) were suspended in PhMe (2 mL) and CHCl₃ (1 mL) and were heated in the microwave to 180 °C (with variable power) for 20 min and then for an additional 10 min. The reaction was then cooled to room temperature, was concentrated, was treated with DCM, and was filtered. The white solid was collected, and the filtrate was concentrated and purified via silica gel chromatography (ISCO column, 40 g, 0 → 5% MeOH/DCM) to afford, after combining with the solid collected earlier, **34** (86 mg, 53%) as a white solid. ¹H NMR (400 MHz, CDCl₃, δ): 10.77 (br s, 1H), 8.52 (d, J = 5.3 Hz, 1H), 8.22 (s, 1H), 7.74 (dd, J = 11.4 Hz, 2.1 Hz, 1H), 7.59 (s, 1H), 7.60–7.55 (m, 1H), 7.45 (s, 1H), 7.43–7.30 (m, 6H), 6.51 (d, J = 5.3 Hz, 1H), 4.09 (s, 2H), 4.08 (s, 3H), 4.07 (s, 3H). MS (ES) m/z : 484 (M + H⁺). HRMS calcd for C₂₈H₂₃FN₃O₄ (M + H⁺), 484.1673; found, 484.1649. Analytical HPLC: 96.9%. t_R = 1.66.

2-Benzyl-5-(4-(6,7-dimethoxyquinolin-4-yl-oxy)-3-fluorophenyl)-6-methylpyrimidin-4(3H)-one (35). By following the procedure that was used to prepare **34**, we prepared compound **35** from phenol **33** in 24% yield as a white solid. ¹H NMR (400 MHz, CDCl₃, δ): 8.49 (d, J = 5.1 Hz, 1H), 7.60 (s, 1H), 7.45 (s, 1H), 7.42–7.26 (m, 8H), 7.19 (d, J = 8.2 Hz, 1H), 6.53 (d, J = 5.1 Hz, 1H), 4.07 (s, 3H), 4.06 (s, 3H), 3.96 (s, 2H), 2.34 (s, 3H). MS (ES) m/z : 498 (M + H⁺). HRMS calcd for C₂₉H₂₅FN₃O₄ (M + H⁺), 498.1829; found, 498.1812. Analytical HPLC: 95.2%. t_R = 2.36.

2-Benzyl-5-(4-(6,7-dimethoxyquinolin-4-yl-oxy)-3-fluorophenyl)-3-methylpyrimidin-4(3H)-one (7). Compound **34** (25 mg, 0.052 mmol) was dissolved in DMF, and K₂CO₃ (11 mg, 0.080 mmol) and MeI (0.004 mL, 0.06 mmol) were added. The reaction was stirred at 43 °C (oil bath temperature) for 2 h, was diluted with DCM, and was washed with water twice and with brine once. The organic layer was dried over sodium sulfate, was filtered, was concentrated, and was purified on silica gel chromatography (ISCO column, 12 g, 0 → 5% MeOH/DCM) to afford a 6:1 mixture of **7** and the undesired O-methylated isomer (11 mg, 42% total yield). This mixture was purified via HPLC (70 → 100% MeCN/water

with 0.1% TFA) to afford pure **7**. ¹H NMR (400 MHz, CDCl₃, δ): 8.52 (d, J = 5.3 Hz, 1H), 8.16 (s, 1H), 7.73 (dd, J = 11.7, 2.1 Hz, 1H), 7.60 (s, 1H), 7.57 (dd, J = 9.4, 0.9 Hz, 1H), 7.45 (s, 1H), 7.42–7.25 (m, 6H), 6.51 (dd, J = 6.8, 0.8 Hz, 1H), 4.23 (s, 2H), 4.08 (s, 3H), 4.07 (s, 3H), 3.56 (s, 3H). MS (ES) m/z : 498 (M + H⁺). Anal. Calcd for (C₂₉H₂₄FN₃O₄·0.1CH₂Cl₂): C, H, N.

2-(Bromo(phenyl)methyl)-5-(4-(6,7-dimethoxyquinolin-4-yloxy)-3-fluorophenyl)-3-methylpyrimidin-4(3H)-one (36). Compound **7** (300 mg, 0.604 mmol) was diluted with CHCl₃, and NBS (0.24 g, 1.3 mmol) was added. The reaction was heated at reflux for 3 h, and then more NBS (53 mg, 0.30 mmol) was added. After another 2 h, the reaction was cooled to room temperature, was concentrated, and was purified via column chromatography (0 → 5% MeOH/DCM). A second column chromatography was necessary that used EtOAc as the eluent to afford pure **36** (113 mg, 32%) as a tan solid. ¹H NMR (400 MHz, CDCl₃, δ): 8.44 (d, J = 5.3 Hz, 1H), 8.09 (s, 1H), 7.65 (dd, J = 11.6, 2.0 Hz, 1H), 7.50 (s, 1H), 7.51–7.43 (m, 3H), 7.41 (s, 1H), 7.38–7.28 (m, 3H), 7.25–7.18 (m, 1H), 6.43 (d, J = 5.3 Hz, 1H), 6.13 (s, 1H), 3.97 (s, 6H), 3.55 (s, 3H). MS (ES) m/z : 576 (Br79, M + H⁺), 578 (Br81, M + H⁺).

2-(Amino(phenyl)methyl)-5-(4-(6,7-dimethoxyquinolin-4-yloxy)-3-fluorophenyl)-3-methylpyrimidin-4(3H)-one (37). Compound **36** (130 mg, 0.226 mmol) was dissolved in DMF (3 mL) and was cooled to 0 °C. NaN₃ (18 mg, 0.28 mmol) was added, and the reaction was stirred for 1 h. It was then concentrated, treated with CHCl₃ and DCM, washed with water, and dried over sodium sulfate. The organic phase was decanted and concentrated and was taken directly to the next step.

The crude material was diluted with EtOAc and THF, and Pd–C (10% by weight, 24 mg) was added. The reaction was then stirred under a balloon of hydrogen for 4.5 h, was flushed with nitrogen, and was filtered through a pad of celite. The filtrate was concentrated and purified via silica gel chromatography (ISCO aminopropyl column, 40 g, 0 → 5% MeOH/DCM) to afford **37** (31 mg, 27% yield over two steps) as a yellow oil. ¹H NMR (400 MHz, CDCl₃, δ): 8.51 (d, J = 5.0 Hz, 1H), 8.41 (s, 1H), 7.93 (dd, J = 12.3, 1.8 Hz, 1H), 7.76 (d, J = 8.5 Hz, 1H), 7.54 (s, 1H), 7.51 (t, J = 8.8 Hz, 1H), 7.44–7.34 (m, 5H), 7.32–7.27 (m, 1H), 6.53 (d, J = 5.0 Hz, 1H), 5.31 (s, 1H), 3.96 (s, 6H), 3.50 (s, 3H), 2.73 (br s, 2H). MS (ES) m/z : 513 (M + H⁺). Anal. Calcd for (C₂₉H₂₅FN₄O₄·0.5CH₂Cl₂): C, H, N.

General Procedure for the Synthesis of 38–41. N-((5-(4-(6,7-Dimethoxyquinolin-4-yl-oxy)-3-fluorophenyl)-1-methyl-6-oxo-1,6-dihydropyrimidin-2-yl)(phenyl)methyl)-2-(dimethylamino)acetamide (38). Amine **37** (25 mg, 0.049 mmol) was diluted with DCM and was cooled in an ice-water bath. Et₃N (0.034 mL, 0.25 mmol) and 2-(dimethylamino)acetyl chloride hydrochloride salt (9 mg, 0.06 mmol) were added, and the reaction was stirred at room temperature until TLC analysis indicated a complete reaction. More Et₃N and 2-(dimethylamino)acetyl chloride hydrochloride salt were added as needed to afford a complete reaction. Upon completion, the reaction was concentrated and purified via silica gel chromatography (ISCO column, 12 g, 0 → 5% MeOH/DCM) to afford **38** (14 mg, 48% yield) as a tan solid. ¹H NMR (400 MHz, CDCl₃, δ): 8.57 (d, J = 8.3 Hz, 1H), 8.52 (d, J = 5.3 Hz, 1H), 8.23 (s, 1H), 7.73 (dd, J = 11.6, 2.0 Hz, 1H), 7.59 (s, 1H), 7.60–7.55 (m, 1H), 7.46 (s, 1H), 7.43–7.35 (m, 5H), 7.32 (t, J = 8.4 Hz, 1H), 6.51 (d, J = 5.3 Hz, 1H), 6.34 (d, J = 8.3 Hz, 1H), 4.07 (s, 3H), 4.06 (s, 3H), 3.54 (s, 3H), 3.01 (s, 2H), 2.32 (s, 6H). MS (ES) m/z : 598 (M + H⁺). HRMS calcd for C₃₃H₃₃FN₅O₅ (M + H⁺), 598.2466; found, 598.2444. Analytical HPLC: 96.9%. t_R = 2.43.

N-((5-(4-(6,7-Dimethoxyquinolin-4-yloxy)-3-fluorophenyl)-1-methyl-6-oxo-1,6-dihydropyrimidin-2-yl)(phenyl)methyl)-propionamide (39). By using propionyl chloride, and by following the procedure that was used to prepare **38**, we obtained **39** (51%) as an off-white solid. ¹H NMR (300 MHz, CDCl₃, δ): 8.52 (d, J = 5.3 Hz, 1H), 8.18 (s, 1H), 7.71 (dd, J = 11.6 Hz, 2.0 Hz, 1H), 7.59 (s, 1H), 7.60–7.54 (m, 1H), 7.44 (s, 1H), 7.42–7.31 (m, 6H), 7.30–7.24 (m, 1H), 6.51 (dd, J = 5.3, 0.7 Hz, 1H), 6.31 (d, J = 7.6 Hz, 1H), 4.07 (s, 3H), 4.06 (s, 3H), 3.52 (s, 3H), 2.31 (dq, J =

7.8, 1.5 Hz, 2H), 1.18 (t, $J = 7.5$ Hz, 3H). MS (ES) m/z : 569 (M + H⁺). Anal. Calcd for (C₃₂H₂₉FN₄O₅·0.2CH₂Cl₂): C, H, N.

N-((5-(4-(6,7-Dimethoxyquinolin-4-yloxy)-3-fluorophenyl)-1-methyl-6-oxo-1,6-dihydropyrimidin-2-yl)(phenyl)methyl)-3-(methylthio)propanamide (40). By using 3-(methylthio)propanoyl chloride, and by following the procedure that was used to prepare **38**, we obtained **40** (47%) as an off-white solid. ¹H NMR (300 MHz, CDCl₃, δ): 8.53 (d, $J = 5.3$ Hz, 1H), 8.18 (s, 1H), 7.72 (dd, $J = 11.6$ Hz, 2.1, 1H), 7.59 (s, 1H), 7.59–7.54 (m, 1H), 7.53–7.47 (m, 1H), 7.48 (s, 1H), 7.42–7.37 (m, 5H), 7.32 (t, $J = 8.3$ Hz, 1H), 6.51 (d, $J = 5.3$ Hz, 1H), 6.30 (d, $J = 7.5$ Hz, 1H), 4.07 (s, 3H), 4.06 (s, 3H), 3.52 (s, 3H), 2.84–2.77 (m, 2H), 2.61–2.55 (m, 2H), 2.09 (s, 3H). MS (ES) m/z : 615 (M + H⁺). HRMS calcd for C₃₃H₃₂FN₄O₅S (M + H⁺), 615.2077; found, 615.2067. Analytical HPLC: 96.2%. $t_R = 1.87$.

3-((5-(4-(6,7-Dimethoxyquinolin-4-yloxy)-3-fluorophenyl)-1-methyl-6-oxo-1,6-dihydro-pyrimidin-2-yl)(phenyl)methyl)-1,1-dimethyl-urea (41). By using dimethylcarbamic chloride, and by following the procedure that was used to prepare **38**, we obtained **41** as an off-white solid. ¹H NMR (300 MHz, CDCl₃, δ): 8.53 (d, $J = 5.1$ Hz, 1H), 8.19 (s, 1H), 7.72 (dd, $J = 11.6$ Hz, 2.0, 1H), 7.59 (s, 1H), 7.60–7.55 (m, 1H), 7.45 (s, 1H), 7.42–7.36 (m, 5H), 7.31 (t, $J = 8.3$ Hz, 1H), 6.51 (d, $J = 5.1$ Hz, 1H), 6.26–6.22 (m, 1H), 6.19–6.14 (m, 1H), 4.08 (s, 3H), 4.06 (s, 3H), 3.54 (s, 3H), 2.96 (s, 6H). MS (ES) m/z : 584 (M + H⁺). Anal. Calcd for (C₃₂H₃₀FN₅O₅·0.3CH₂Cl₂): C, H, N.

General Procedure for the Synthesis of 42, 43, and 51. **2-(4-Methylbenzyl)-5-(3-fluoro-4-(6-methoxy-7-(3-morpholinopropoxy)quinolin-4-yloxy)phenyl)-3-methylpyrimidin-4(3H)-one (42)**. 4-Chloro-6-methoxy-7-(3-morpholinopropoxy)quinoline (**16**, 116.7 mg, 0.346 mmol), 2-(4-methylbenzyl)-5-(3-fluoro-4-hydroxyphenyl)-3-methylpyrimidin-4(3H)-one (**12**, 120.6 mg, 0.372 mmol), copper powder (9.8 mg, 0.15 mmol), and solid KOH (56.1 mg, 1.0 mmol) were suspended in DMF (1 mL) and pyridine (1 mL) and were heated in the CEM microwave to 110 °C at 110 W for 18 min. The reaction was cooled to room temperature. We ran five more reactions in the microwave by using the same reagents in approximately the same amounts. For all six runs, the total amounts of **16** and **12** used were 1.164 g (3.457 mmol) and 1.417 g (4.370 mmol), respectively. Once completed, all six reactions were combined and were poured into 1 N NaOH (39 mL), which was then diluted with DCM. The layers were separated, and the aqueous phase was extracted repeatedly with DCM. The organic phases were combined, were dried over sodium sulfate, were filtered, were concentrated, and were purified on HPLC (1 → 70% MeCN/water with 0.1% TFA over 55–65 min). The fractions with product were collected, were concentrated, and were re-purified on HPLC (10 → 95% MeCN/water with 0.1% TFA). The fractions with product were collected, were concentrated, were diluted with DCM (~5 mL), and were treated with polymer-supported carbonate (560 mg, MP-carbonate, Argonaut Aquatics, 2.75 mmol/g). The suspension was stirred for 75 min and was then filtered. The filtrate was concentrated and was dried under high vacuum to afford **42** (115.0 mg, 5%) as a rust-colored solid. ¹H NMR (400 MHz, CDCl₃, δ): 8.53 (d, $J = 5.5$ Hz, 1H), 8.16 (s, 1H), 7.74 (dd, $J = 9.6$, 2.0 Hz, 1H), 7.60 (s, 1H), 7.60–7.52 (m, 2H), 7.32 (t, $J = 8.3$ Hz, 1H), 7.21–7.13 (m, 4H), 6.54 (d, $J = 5.5$ Hz, 1H), 4.30 (t, $J = 6.5$ Hz, 2H), 4.19 (s, 2H), 4.06 (s, 3H), 3.83–3.78 (m, 4H), 3.56 (s, 3H), 2.80–2.60 (m, 6H), 2.36 (s, 3H), 2.25–2.17 (m, 2H). MS (ES) m/z : 625 (M + H⁺). Anal. Calcd for (C₃₆H₃₇FN₄O₅·0.6CH₂Cl₂): C, H, N.

2-(4-Fluorobenzyl)-5-(3-fluoro-4-(6-methoxy-7-(3-morpholinopropoxy)quinolin-4-yloxy)phenyl)-3-methylpyrimidin-4(3H)-one (43). By using phenol **13**, and by following the procedure that was used to prepare **42**, we obtained **43** (1%) as a rust-colored solid. ¹H NMR (400 MHz, *d*₆-DMSO, δ): 8.50 (d, $J = 5.3$ Hz, 1H), 8.27 (s, 1H), 7.91 (dd, $J = 12.5$, 2.0 Hz, 1H), 7.73 (d, $J = 8.4$ Hz, 1H), 7.53 (s, 1H), 7.50 (t, $J = 8.6$ Hz, 1H), 7.42 (s, 1H), 7.34 (dd, $J = 8.5$, 5.8 Hz, 2H), 7.19 (t, $J = 8.9$ Hz, 2H), 6.51 (d, $J = 5.3$ Hz, 1H), 4.27 (s, 2H), 4.21 (t, $J = 6.5$ Hz, 2H), 3.95 (s, 3H), 3.59 (t, $J = 4.5$ Hz, 4H), 3.54 (s, 3H), 2.50–2.44 (m, 2H),

2.42–2.37 (m, 4H), 1.98 (qn, $J = 6.0$ Hz, 2H). MS (ES) m/z : 629 (M + H⁺). Anal. Calcd for (C₃₅H₃₄F₂N₄O₅·0.2CH₂Cl₂) C, H, N: Found, 65.90; Calcd, 65.48.

5-(3-Fluoro-4-(6-methoxy-7-(3-morpholino-propoxy)quinolin-4-yloxy)phenyl)-2-(4-fluorophenylamino)-3-methylpyrimidin-4(3H)-one (51). By using phenol **47**, and by following the procedure that was used to prepare **42**, we obtained **51** (6%) as a tan solid. ¹H NMR (400 MHz, *d*₆-DMSO, δ): 9.06 (s, 1H), 8.49 (d, $J = 5.3$ Hz, 1H), 8.09 (s, 1H), 7.87 (dd, $J = 12.8$, 1.7 Hz, 1H), 7.67 (d, $J = 8.8$ Hz, 1H), 7.57–7.51 (m, 3H), 7.46–7.39 (m, 2H), 7.22 (t, $J = 8.8$ Hz, 2H), 6.49 (d, $J = 5.1$ Hz, 1H), 4.21 (t, $J = 5.7$ Hz, 2H), 3.95 (s, 3H), 3.63–3.57 (m, 4H), 3.57 (s, 3H), 2.50–2.35 (m, 6H), 2.06–1.93 (m, 2H). MS (ES) m/z : 630 (M + H⁺). Anal. Calcd for (C₃₄H₃₃F₂N₅O₅·0.4CH₂Cl₂): C, H, N.

5-(3-Fluoro-4-hydroxyphenyl)-3-methyl-2-(methylthio)pyrimidin-4(3H)-one (44). Compound **10** (10.0 g, 35.8 mmol) was dissolved in HOAc (60 mL) and 48% aqueous HBr (240 mL). The flask was equipped with a reflux condenser and was placed in a preheated oil bath (115–120 °C) and was stirred for 3 h. The reaction was then cooled to room temperature and was poured into a 2 L Erlenmeyer flask. Saturated NaHCO₃ (1.3 L) was added in portions over 1 h, and the solution was stirred overnight at room temperature. Then, 5 N NaOH (100 mL) was added, and stirring was continued for 20 min. The suspension was filtered, and the solid was collected and dried under high vacuum at 60 °C to afford **44** (9.8 g, ~100%) as a white solid. ¹H NMR (400 MHz, CDCl₃, δ): 7.95 (s, 1H), 7.51 (dd, $J = 11.9$, 2.0 Hz, 1H), 7.30–7.25 (m, 1H), 7.02 (t, $J = 8.8$ Hz, 1H), 5.33 (br s, 1H), 3.61 (s, 3H), 2.65 (s, 3H). MS (ES) m/z : 267 (M + H⁺).

General Procedure for the Synthesis of 48–50. **5-(4-(6,7-Dimethoxyquinolin-4-yloxy)-3-fluorophenyl)-3-methyl-2-(phenylamino)pyrimidin-4(3H)-one (48)**. Phenol **44** (508.1 mg, 1.908 mmol) was suspended in aniline (4.5 mL), and concentrated HCl (3 drops) was added. The suspension was sealed in a microwave vial and was heated in the CEM microwave to 120 °C at 100 W for 10 min. The reaction was diluted with EtOAc (~100 mL) and was washed with 1 N NaOH (3 × 25 mL). The aqueous washings were combined and were extracted with EtOAc (10 mL). This EtOAc extraction was washed with 1 N NaOH (20 and 10 mL). Finally, all of the aqueous extractions were combined, were washed with Et₂O (3 × 15 mL), and were treated with 1 N HCl to lower the pH to about 8. The aqueous phase was extracted with EtOAc, and these organic extracts were combined and were washed with water (3 × 10 mL) and 1 N NaOH. The pH of these aqueous washings was adjusted with to be around 6 by concentrated HCl and then 1 N NaOH, and this aqueous phase was extracted with EtOAc and Et₂O. These organic extracts were combined, were dried over sodium sulfate, were filtered, were concentrated, and were dried under high vacuum to afford phenol **45** (466.1 mg, 78%).

Phenol **45** (210.3 mg, 0.6756 mmol), 4-chloro-6,7-dimethoxyquinoline (247.2 mg, 1.106 mmol), and DMAP (29.8 mg, 0.244 mmol) were suspended in 1,4-dioxane (4.0 mL) and were heated in the CEM microwave to 120 °C at 300 W for 20 min. The reaction was briefly cooled and was then reheated under the same conditions for 15 min. The reaction was cooled to room temperature once more, was concentrated, and was purified via HPLC (10 → 95% MeCN/water with 0.1% TFA). The fractions with product were collected, were concentrated, and were filtered through a plug of silica gel with EtOAc and then with 5% MeOH/EtOAc. The filtrate was concentrated and was again filtered through silica gel with EtOAc. Fractions with product were collected, were concentrated, and were dried under high vacuum to afford **48** (20.9 mg, 6%). For analytical purposes, a 4 mg aliquot was purified on a pipet silica gel column (50:1 → 25:1 DCM/MeOH) to afford analytically pure material. ¹H NMR (400 MHz, CDCl₃, δ): 8.50 (d, $J = 5.3$ Hz, 1H), 7.97 (s, 1H), 7.66 (dd, $J = 11.9$, 2.0 Hz, 1H), 7.60 (s, 1H), 7.52–7.38 (m, 7H), 7.25–7.20 (m, 2H), 6.51 (dd, $J = 5.3$, 1.0 Hz, 1H), 4.07 (s, 3H), 4.05 (s, 3H), 3.69 (s, 3H). MS (ES) m/z : 499 (M + H⁺). HRMS calcd for C₂₈H₂₄FN₄O₄ (M + H⁺), 499.1782; found, 499.1767. Analytical HPLC: 96.6%. $t_R = 1.74$.

5-(4-(6,7-Dimethoxyquinolin-4-yloxy)-3-fluorophenyl)-2-(2-fluorophenylamino)-3-methylpyrimidin-4(3H)-one (49). By using phenol **46** (prepared in the same manner as **45** above) and 4-chloro-6,7-dimethoxyquinoline, and by following the procedure that was used to prepare **48**, we obtained **49** (1%) as an off-white solid. ¹H NMR (400 MHz, *d*₆-DMSO, δ): 9.12 (s, 1H), 8.57 (s, 1H), 8.05 (s, 1H), 7.87 (d, *J* = 12.5 Hz, 1H), 7.73–7.22 (m, 8H), 6.61 (s, 1H), 3.97 (s, 6H), 3.58 (s, 3H). MS (ES) *m/z*: 517 (M + H⁺). HRMS calcd for C₂₈H₂₃F₂N₄O₄ (M + H⁺), 517.1687; found, 517.1667. Analytical HPLC: 98.1%. *t*_R = 2.27.

5-(4-(6,7-Dimethoxyquinolin-4-yloxy)-3-fluorophenyl)-2-(4-fluorophenylamino)-3-methylpyrimidin-4(3H)-one (50). By using phenol **47** (prepared in the same manner as **45** above) and 4-chloro-6,7-dimethoxyquinoline, and by following the procedure that was used to prepare **48**, we obtained **50** (6%) as an off-white solid. ¹H NMR (400 MHz, *d*₆-DMSO, δ): 9.06 (s, 1H), 8.66 (s, 1H), 8.12 (s, 1H), 7.92 (d, *J* = 13.1 Hz, 1H), 7.73 (d, *J* = 9.8 Hz, 1H), 7.68–7.63 (m, 1H), 7.53–7.47 (m, 3H), 7.51–7.47 (m, 1H), 7.23 (t, *J* = 8.9 Hz, 2H), 6.74 (m, 1H), 4.00 (s, 6H), 3.57 (s, 3H). MS (ES) *m/z*: 517 (M + H⁺). HRMS calcd for C₂₈H₂₃F₂N₄O₄ (M + H⁺), 517.1687; found, 517.1670. Analytical HPLC: 95.1%. *t*_R = 2.24.

5-(4-(6,7-Dimethoxyquinolin-4-yloxy)-3-fluorophenyl)-3-methyl-2-(methylthio)-pyrimidin-4(3H)-one (52). Phenol **44** (2.82 g, 10.6 mmol), 4-chloro-6,7-dimethoxyquinoline (2.10 g, 9.40 mmol), and DMAP (110.1 mg, 0.901 mmol) were suspended in pyridine (30 mL) and 1,4-dioxane (15 mL), and the reaction flask was heated in an oil bath (110 °C) while the reaction was stirred under argon overnight. The reaction was cooled to room temperature, was diluted with water (75 mL), and was filtered. The solid was washed with water and was dried under high vacuum to afford **52** (2.50 g, 59%). ¹H NMR (400 MHz, *d*₆-DMSO, δ): 8.50 (d, *J* = 5.1 Hz, 1H), 8.29 (s, 1H), 7.90 (dd, *J* = 12.4, 1.7 Hz, 1H), 7.72 (d, *J* = 8.8 Hz, 1H), 7.54 (s, 1H), 7.50 (t, *J* = 8.6 Hz, 1H), 7.42 (s, 1H), 6.52 (d, *J* = 5.3 Hz, 1H), 3.95 (s, 6H), 3.52 (s, 3H), 2.62 (s, 3H). MS (ES) *m/z*: 454 (M + H⁺).

5-(4-(6,7-Dimethoxyquinolin-4-yloxy)-3-fluorophenyl)-2-hydroxy-3-methylpyrimidin-4(3H)-one (53). Compound **52** (8.90 g, 19.6 mmol) was dissolved in a solution of MeCN (288 mL) and TFA (32 mL), which was then cooled to –5 °C in a dilute dry-ice/acetone bath. Urea hydrogen peroxide (7.37 g, 78.4 mmol) was added, and the reaction was stirred for 5 min. TFAA (10.90 mL, 78.40 mmol) was added dropwise via a dropping funnel while the temperature was maintained at –5 °C. The reaction was stirred at this temperature for 30 min and was then allowed to warm up to room temperature, where it was stirred for 3 h. The reaction was then diluted with DCM and H₂O, and the layers were separated. The aqueous phase was extracted with DCM, and the organic phases were combined, were dried over sodium sulfate, were filtered, were concentrated, and were dried in vacuo at 100 °C over the weekend to afford **53** (10.00 g, 95% yield) as a beige solid. ¹H NMR (300 MHz, CDCl₃, δ): 10.50 (d, *J* = 5.4 Hz, 1H), 8.70 (d, *J* = 6.6 Hz, 1H), 7.86 (s, 1H), 7.69 (s, 1H), 7.69–7.55 (m, 2H), 7.49 (d, *J* = 8.5 Hz, 1H), 7.36 (t, *J* = 8.3 Hz, 1H), 6.80 (d, *J* = 6.1 Hz, 1H), 4.15 (s, 3H), 4.13 (s, 3H), 3.42 (s, 3H). MS (ES) *m/z*: 424 (M + H⁺).

General Procedure for the Synthesis of 55 and 56. **5-(4-(6,7-Dimethoxyquinolin-4-yloxy)-3-fluorophenyl)-2-(3-fluorophenylamino)-3-methylpyrimidin-4(3H)-one (55).** Compound **53** (~240 mg, 0.57 mmol) was dissolved in POCl₃ (16 mL) and *N,N*-dimethylaniline (1.6 mL). The reaction was heated to 125 °C for 8.5 h and was then cooled to room temperature and was stirred overnight. It was then concentrated and diluted with DCM (~125 mL). The organic phase was washed with saturated sodium bicarbonate (25 and 17 mL), was dried over sodium sulfate, was filtered, and was concentrated. Crude chloride **54** was dissolved in 1,4-dioxane (15 mL) and was used for the next step.

This solution (5 mL) was put in a microwave vial, and 3-fluoroaniline (0.2 mL, 2 mmol) and concentrated HCl (1 drop) were added. The vial was sealed and was heated in the CEM microwave to 60 °C at 60 W for 5 min. The reaction was then cooled to room temperature, was concentrated, and was filtered

through a plug of silica gel (EtOAc, 2:1 EtOAc/MeOH → 3:2 MeOH/EtOAc). The filtrate was concentrated and was purified on HPLC (10 → 95% MeCN/water with 0.1% TFA). The fractions with product were collected, were concentrated, and were purified two times on a silica gel plug (EtOAc → 1% MeOH/EtOAc the first time, EtOAc the second time) to afford **55** (14.4 mg) as a light-yellow solid. ¹H NMR (400 MHz, *d*₆-DMSO, δ): 9.14 (s, 1H), 8.59 (d, *J* = 5.5 Hz, 1H), 8.17 (s, 1H), 7.91 (d, *J* = 13.6 Hz, 1H), 7.72 (d, *J* = 8.5 Hz, 1H), 7.60 (s, 1H), 7.60–7.53 (m, 1H), 7.51–7.38 (m, 4H), 7.00–6.94 (m, 1H), 6.63 (d, *J* = 5.0 Hz, 1H), 3.96 (s, 6H), 3.59 (s, 3H). MS (ES) *m/z*: 517 (M + H⁺). HRMS calcd for C₂₈H₂₃F₂N₂O₄ (M + H⁺), 517.1687; found, 517.1672. Analytical HPLC: 95.0%. *t*_R = 6.37.

5-(4-(6,7-Dimethoxyquinolin-4-yloxy)-3-fluorophenyl)-3-methyl-2-(4-(trifluoro-methyl)phenylamino)pyrimidin-4(3H)-one (56). By using 5 mL of the same solution of crude chloride **54**, and by following the procedure that was used to prepare **55**, we obtained **56** (12.8 mg) as a light-yellow solid. ¹H NMR (400 MHz, *d*₆-DMSO, δ): 9.30 (s, 1H), 8.50 (d, *J* = 5.5 Hz, 1H), 8.15 (s, 1H), 7.93–7.82 (m, 3H), 7.75–7.68 (m, 3H), 7.54 (s, 1H), 7.46 (t, *J* = 8.5 Hz, 1H), 7.42 (s, 1H), 6.52 (d, *J* = 5.0 Hz, 1H), 3.96 (s, 6H), 3.61 (s, 3H). MS (ES) *m/z*: 567 (M + H⁺). HRMS calcd for C₂₉H₂₃F₄N₄O₄ (M + H⁺), 567.1655; found, 567.1638. Analytical HPLC: 95.5%. *t*_R = 6.96.

5-(Benzyloxy)-2-bromopyridine (57). A suspension of sodium hydride (3.808 g, Aldrich 60%, 95.20 mmol) and DMF (25 mL) was cooled in an ice-water bath under nitrogen, and 2-bromo-5-hydroxypyridine (14.28 g, 82.07 mmol) was added via syringe as a solution in DMF (120 mL) over 35 min. The reaction was warmed to room temperature, was stirred under nitrogen for 40 min, and was then cooled again in an ice-water bath. Benzyl bromide (12.0 mL, 98 mmol) was added via syringe, and the reaction was warmed to room temperature and was stirred for 90 min. It was then poured into 2.5% aqueous HCl (400 mL), and the pH of the aqueous layer was raised to 14 with 5 N NaOH and was then lowered to 12 with concentrated HCl, which caused precipitation. The solution was decanted, and the decanted liquid was extracted with EtOAc (3 × 300 mL). Organic extracts were combined, were dried over sodium sulfate, were filtered, and were concentrated. The concentrate and the precipitate were combined, were diluted with EtOAc (~400 mL), and were washed with water (3 × 150 mL). The organic phase was dried over sodium sulfate, was filtered, was concentrated, and was filtered through a 2in silica gel with EtOAc. The filtrate was concentrated and was dried under high vacuum to afford **57** (22.9 g). ¹H NMR (400 MHz, CDCl₃, δ): 8.14 (d, *J* = 3.1 Hz, 1H), 7.43–7.35 (m, 6H), 7.16 (dd, *J* = 8.6, 3.1 Hz, 1H), 5.10 (s, 2H). MS (ES) *m/z*: 264 (Br79, M + H⁺), 266 (Br81, M + H⁺).

2-(5-(Benzyloxy)pyridin-2-yl)acetic Acid (58). **57** (22.9 g, 86.7 mmol) and Pd(PPh₃)₄ (11.3 g, 9.78 mmol) were dissolved in THF (100 mL). Argon was bubbled through for 5 min, and then 2-*tert*-butoxy-2-oxoethylzinc chloride (199 mL, 0.5 M in Et₂O, 99.5 mmol) was added via syringe. The flask was equipped with a reflux condenser and was placed in a preheated oil bath (60 °C) and was stirred under argon. After 4 h, more Pd(PPh₃)₄ (0.62 g, 0.54 mmol) was added. Stirring was continued at reflux for 1 h, and then the reaction was cooled to room temperature and was quenched with 250 mL of a 1:1 solution of saturated ammonium chloride and saturated EDTA (disodium salt). The layers were separated, and the aqueous phase was extracted with EtOAc (200 mL). The organic extracts were combined, were dried over sodium sulfate, were filtered, and were concentrated. After the mixture sat at room temperature overnight, a precipitate formed, so the suspension was refiltered, and the filtrate was concentrated and was filtered through a 2in silica gel with 5:1 → 2:1 hexanes/EtOAc → EtOAc.

The filtrate was concentrated, was dissolved in DCM (250 mL), and was cooled to 0 °C in an ice-water bath under argon. TFA (30 mL, 404 mmol) was added via syringe, and the reaction was allowed to warm to room temperature while being stirring overnight.

The next morning, an additional 30 mL of TFA was added, and stirring was continued at room temperature. After 5 h, the reaction was concentrated, was poured into 10% aqueous sodium carbonate

(200 mL), and was diluted with DCM (150 mL). More 10% aqueous sodium carbonate (100 mL) was added, and the layers were separated. The aqueous layer was washed with DCM (2×150 mL), and the organic extracts were then extracted with 10% aqueous sodium carbonate (100 mL) and 1 N NaOH (50 mL). All aqueous phases and extractions were combined, and the pH was lowered to about 8 by concentrated HCl, which caused precipitation. This suspension was filtered, and the pH of the filtrate was lowered to about 4 by concentrated HCl, which caused more precipitation. This suspension was also filtered, and the solid was allowed to dry in the air for ~ 3 days and was then dried under high vacuum at 60 °C to afford **58** (11.323 g, 57% over 3 steps). $^1\text{H NMR}$ (400 MHz, d_6 -DMSO, δ): 12.50–12.21 (br s, 1H), 8.24 (d, $J = 3.0$ Hz, 1H), 7.48–7.30 (m, 6H), 7.27 (d, $J = 8.5$ Hz, 1H), 5.17 (s, 2H), 3.66 (s, 2H). MS (ES) m/z : 244 ($M + \text{H}^+$).

5-(5-(Benzyloxy)pyridin-2-yl)-3-methyl-2-(methylthio)pyrimidin-4(3H)-one (60). Acid **58** (11.323 g, 46.55 mmol) was suspended in DCM (200 mL), and DMF (0.25 mL) was added. Then, $(\text{COCl})_2$ (4.5 mL, 52 mmol) was added dropwise via syringe over 25 min, which caused vigorous gas evolution. The reaction was stirred at room temperature for about 10 min, and salt **59** (15.71 g, 54.74 mmol) was added. The suspension was cooled to 0 °C, triethylamine (23.0 mL, 165 mmol) was added via syringe, and DCM (3.5 mL) was added to rinse the sides of the flask. The solution was allowed to warm to room temperature and was stirred for 41 h. The reaction was then quenched with water (175 mL), and the layers were separated. The aqueous phase was extracted with DCM (2×150 mL), and the organic extracts and phases were combined, were dried over MgSO_4 , were filtered, were concentrated, and were filtered through silica gel (~ 2 in) with DCM \rightarrow 100:1 \rightarrow 10:1 DCM/MeOH. The fractions with product were collected, were concentrated, and were filtered again through silica gel with DCM \rightarrow 100:1 \rightarrow 10:1 DCM/MeOH. We repeated this process one last time by using an eluent system of DCM \rightarrow 100:1 \rightarrow 50:1 DCM/MeOH. Fractions with product were collected and concentrated, and the solid was washed with hexanes, Et_2O , and EtOAc and was filtered. The solid was collected and was set aside as batch no. 1. The filtrate was collected, concentrated, and refiltered, and the solid was washed with DCM. This filtrate was purified on silica gel (~ 2 in, DCM \rightarrow 50:1 \rightarrow 10:1 \rightarrow 5:1 DCM/MeOH), and the fractions with product were combined with the solid that was set aside earlier (batch no. 1), were concentrated, and were dried under high vacuum to afford **60** (5.21 g, 69% purity, 23% yield). For characterization purposes, a small amount of **60** (prepared separately) was washed with MeOH and acetone and was dried in vacuo. $^1\text{H NMR}$ (400 MHz, CDCl_3 , δ): 8.69 (s, 1H), 8.41 (d, $J = 2.8$ Hz, 1H), 8.32 (d, $J = 8.9$ Hz, 1H), 7.48–7.28 (m, 6H), 5.15 (s, 2H), 3.62 (s, 3H), 2.64 (s, 3H). MS (ES) m/z : 340 ($M + \text{H}^+$).

2-(4-Fluorophenylamino)-5-(5-(6-methoxy-7-(3-morpholinopropoxy)quinolin-4-yloxy)-pyridin-2-yl)-3-methylpyrimidin-4(3H)-one (62). A 100 mL round-bottomed flask was charged with **60** (1.05 g, 3.09 mmol) and 1,4-dioxane (25 mL). Then, 4-fluoroaniline (1.5 mL, 16 mmol) and concentrated HCl (0.04 mL, 1 mmol) were added, and the flask was fit with a reflux condenser, was put in a preheated oil bath (120–125 °C), and was stirred under nitrogen. After 1 day, 1.5 mL of 4-fluoroaniline was added, and stirring was continued at reflux for 1 week total. The reaction was then cooled to room temperature, was concentrated, and was filtered through 2 in of silica gel with DCM \rightarrow 20:1 DCM/MeOH. Fractions with product were collected, were concentrated, and were taken to the next step.

The material was diluted with DCM (20 mL) and BBR_3 (4.0 mL, 1.0 M in DCM, 4.0 mmol) was added via syringe, which caused precipitation to occur. The flask was placed in a water bath, was stirred under argon for 45 min, and was then quenched with saturated NaHCO_3 (40 mL). The aqueous phase was extracted with 10:1 DCM/MeOH (4×100 mL, 50 mL) and 4:1 DCM/MeOH (2×150 mL, 50 mL, 150 mL), and the organic extracts were combined, were dried over sodium sulfate and magnesium sulfate, were filtered, and were concentrated to afford phenol **61** (1.157 g, 53% purity, 63% yield over 2 steps).

Phenol **61** (574 mg, 1.84 mmol), chloride **16** (458.9 mg, 1.36 mmol), and DMAP (20.9 mg, 0.18 mmol) were dissolved in pyridine (4.6 mL) and 1,4-dioxane (2.3 mL) in a 50 mL round-bottomed flask. The flask was fit with a reflux condenser, was placed in a preheated oil bath (130–135 °C), and was stirred under nitrogen for 5 h.

The reaction was cooled to room temperature, was poured into 1 N NaOH (17 mL), and was extracted with DCM (4×30 mL, 2×50 mL). The organic extracts were combined, were dried over magnesium sulfate, were filtered, were concentrated, and were filtered through silica gel (2 in, 10:1 \rightarrow 5:1 DCM/MeOH \rightarrow 5:1 DCM/2 N ammonia in MeOH). The filtrate was concentrated and was purified on silica gel (20:1 \rightarrow 10:1 DCM/2 N ammonia in MeOH). It was repurified on silica gel (10:1 DCM/2 N ammonia in MeOH) to afford **62** (106.8 mg, 13%) as a light-orange solid. $^1\text{H NMR}$ (400 MHz, CDCl_3 , δ): 8.75 (s, 1H), 8.54–8.51 (m, 2H), 8.47 (d, $J = 8.8$ Hz, 1H), 7.55 (s, 1H), 7.55–7.51 (m, 1H), 7.50–7.45 (m, 3H), 7.13 (t, $J = 8.6$ Hz, 2H), 6.54 (d, $J = 5.3$ Hz, 1H), 6.46 (s, 1H), 4.29 (t, $J = 6.7$ Hz, 2H), 4.04 (s, 3H), 3.75–3.72 (m, 4H), 3.71 (s, 3H), 2.59 (t, $J = 7.1$ Hz, 2H), 2.53–2.47 (m, 4H), 2.15 (qn, $J = 6.8$ Hz, 2H). MS (ES) m/z : 613 ($M + \text{H}^+$). Anal. Calcd for $(\text{C}_{33}\text{H}_{33}\text{FN}_6\text{O}_5 \cdot 0.4\text{CH}_2\text{Cl}_2)$: C, H, N.

c-Met and KDR Enzyme Assays. K_i values for specific compounds were derived from IC_{50} measurements versus the c-Met and KDR kinases that were determined by the use of homogeneous time-resolved fluorescence (HTRF) assays, as previously described.⁴⁴ We tested molecules in a 10-point serial dilution by using an ATP concentration of two-thirds the K_m value that was determined experimentally and was calculated by the use of the Eadie–Hofstee and Lineweaver–Burke methods.

Cell-Based Assays. According to ref 27, PC3 and CT26 cells were obtained from the American Type Culture Collection (ATCC, Rockville, MD). Cells were grown as monolayers by the use of standard cell culture conditions. IC_{50} measurements of compound activities on HGF-mediated c-Met autophosphorylation were determined in serum-starved PC3 (human) or CT26 (mouse) cells by the use of a quantitative electrochemiluminescent immunoassay. Cells were plated at a density of 20 000 cells/well in 96-well plates. After plating (24 h), cells were starved in media that contained 0.1% BSA for 18 to 20 h. Cells were then treated with a 10-point serial dilution of each tested compound for 1 h at 37 °C, followed by stimulation with optimal concentrations of recombinant human HGF for 10 min at 37 °C. Cells were washed once with PBS and were lysed (1% Triton X-100, 50 mM Tris pH 8.0, 100 mM NaCl, 300 μM Na_3OV_4 and protease inhibitors). Cell lysates were incubated with a biotin-labeled goat-anti-c-Met antibody (BAF358 for human and c-Met and BAF527 for mouse, R&D Systems, Minneapolis, MN) for capture, followed by a mouse antiphosphotyrosine antibody 4G10 (Upstate, Charlottesville, VA) and a BV-tag-labeled antimouse IgG (BioVeris, Gaithersburg, MD) as the detection antibody. Levels of c-Met phosphorylation were then measured on a BioVeris M-series instrument. The IC_{50} values are calculated by the use of the Xlfit4-parameter equation.

Pharmacodynamic Assay. According to ref 27, the effect of **22**, **51**, and **62** on HGF-mediated c-Met phosphorylation in vivo was evaluated in the liver of female BALB/c mice. Compounds were administered by either PO or IP at 10, 30, or 100 mg/kg. After a single dose (2 h), 12 μg human HGF was injected *iv* to phosphorylate c-Met in the liver. After HGF injection (5 min), the livers were harvested, and levels of phosphorylated c-Met were determined by a quantitative electrochemiluminescent assay. c-Met phosphorylation that was measured in livers from mice that were injected with BSA and were treated with vehicle served as a negative control and indicated the background level. Livers from mice that were injected with HGF and were treated with vehicle established the maximal level of c-Met phosphorylation in the liver. Statistical significance was evaluated by analysis of variance (ANOVA), followed by the Bonferroni/Dunn post hoc test by the use of StatView software v5.0.1. Data represent the mean ($n = 3$) \pm standard deviation.

Crystallography. Crystals of c-Met were grown as previously described.²⁷ Compounds were dissolved in DMSO to a final concentration of 20 mM and were then mixed with c-Met protein to a final DMSO concentration of 4% prior to crystallization. Crystals were grown from 12% PEG 6K, 1.0 M LiCl₂, and 0.1 M sodium citrate, pH 5.0. Large crystals that were suitable for data collection were obtained by microseeding. Data were collected on a FRE that was equipped with an RaxisII++ and were scaled by the use of the Denzo/Scalepack programs. We solved the structures by molecular replacement by using the published c-Met structure 1RIW as a search model and the program AMORE. The structures were built and refined by the use of COOT and REFMAC. All Figures were prepared by the use of PyMOL.

Acknowledgment. We thank Jean-Christophe Harmange, Ron Hermenau, and Mark Norman for their assistance in preparing this manuscript. We also thank Howie Yu for his assistance in retrieving and compiling analytical data.

Supporting Information Available: Elemental analyses and HPLC methods for key compounds and X-ray data for **7** and **50**. This material is available free of charge via the Internet at <http://pubs.acs.org>.

References

- Longati, P.; Comoglio, P. M.; Bardelli, A. Receptor Tyrosine Kinases as Therapeutic Targets: The Model of the Met Oncogene. *Curr. Drug Targets* **2001**, *2*, 41–55.
- Haddad, R.; Lipson, K. E.; Webb, C. P. Hepatocyte Growth Factor Expression in Human Cancer and Therapy with Specific Inhibitors. *Anticancer Res.* **2001**, *21*, 4243–4252.
- Maulik, G.; Shrikhande, A.; Kijima, T.; Ma, P. C.; Morrison, P. T.; Salgi, R. Role of the Hepatocyte Growth Factor Receptor, c-Met, in Oncogenesis and Potential for Therapeutic Inhibition. *Cytokine Growth Factor Rev.* **2002**, *13*, 41–59.
- Matsumoto, K.; Date, K.; Shimura, H.; Nakamura, T. Acquisition of Invasive Phenotype in Gallbladder Cancer Cells Via Mutual Interaction of Stromal Fibroblasts and Cancer Cells as Mediated by Hepatocyte Growth Factor. *Jpn. J. Cancer Res.* **1996**, *87*, 702–710.
- Jeffers, M.; Rong, S.; Vande Woude, G. F. Enhanced Tumorigenicity and Invasion-Metastasis by Hepatocyte Growth Factor/Scatter Factor-Met Signaling in Human Cells Concomitant with Induction of the Urokinase Proteolysis Network. *Mol. Cell. Biol.* **1996**, *16*, 1115–1125.
- Birchmeier, C.; Birchmeier, W.; Gherardi, E.; Vande Woude, G. F. Met, Metastasis, Motility and More. *Nat. Rev. Mol. Cell Biol.* **2003**, *4*, 915–925.
- Corso, S.; Comoglio, P. M.; Giordano, S. Cancer Therapy: Can the Challenge Be MET? *Trends Mol. Med.* **2005**, *11*, 284–292.
- Ma, P. C.; Maulik, G.; Christensen, J.; Salgia, R. C-Met: Structure, Functions, and Potential for Therapeutic Inhibition. *Cancer Metastasis Rev.* **2003**, *22*, 309–325.
- Christensen, J. G.; Burrows, J.; Salgia, R. c-Met as a Target for Human Cancer and Characterization of Inhibitors for Therapeutic Intervention. *Cancer Lett.* **2005**, *225*, 1–26.
- Dussault, I.; Kaplan-Lefko, P.; Jun, T.; Coxon, A.; Burgess, T. L. HGF- and c-Met-Targeted Drugs: Hopes, Challenges, and their Future in Cancer Therapy. *Drugs Future* **2006**, *31*, 819–825.
- Cao, B.; Su, Y.; Oskarsson, M.; Zhao, P.; Kort, E. J.; Fisher, R. J.; Wang, L. M.; Woude, G. F. V. Neutralizing Monoclonal Antibodies to Hepatocyte Growth Factor/Scatter Factor (HGF/SF) Display Antitumor Activity in Animal Models. *Proc. Natl. Acad. Sci. U.S.A.* **2001**, *98*, 7443–7448.
- Kim, K. J.; Wang, L.; Su, Y. C.; Gillespie, G. Y.; Salhotra, A.; Lal, B.; Laterra, J. Systemic Anti-Hepatocyte Growth Factor Monoclonal Antibody Therapy Induces the Regression of Intracranial Glioma Xenografts. *Clin. Cancer Res.* **2006**, *12*, 1292–1298.
- Burgess, T.; Coxon, A.; Meyer, S.; Sun, J.; Rex, K.; Tsuruda, T.; Chen, Q.; Ho, S. Y.; Li, L.; Kaufman, S.; McDorman, K.; Cattley, R. C.; Sun, J.; Elliot, G.; Zhang, K.; Feng, X.; Jia, X. C.; Green, L.; Radinsky, R.; Kendall, R. Fully Human Monoclonal Antibodies to Hepatocyte Growth Factor with Therapeutic Potential Against Hepatocyte Growth Factor/c-Met-Dependent Human Tumors. *Cancer Res.* **2006**, *66*, 1721–1729.
- Martens, T.; Schmidt, N. O.; Eckerich, C.; Fillbrandt, R.; Merchant, M.; Schwall, R.; Westphal, M.; Lamszus, K. A Novel One-Armed Anti-c-Met Antibody Inhibits Glioblastoma Growth In Vivo. *Clin. Cancer Res.* **2006**, *12*, 6144–6152.
- Date, K.; Matsumoto, K.; Shimura, H.; Tanaka, M.; Nakamura, T. HGF/NK4 is a Specific Antagonist for Pleiotrophic Actions of Hepatocyte Growth Factor. *FEBS Lett.* **1997**, *420*, 1–6.
- Tomioaka, D.; Maehara, N.; Kuba, K.; Mizumoto, K.; Tanaka, M.; Matsumoto, K.; Nakamura, T. Inhibition of Growth, Invasion, and Metastasis of Human Pancreatic Carcinoma Cells by NK4 in an Orthotopic Mouse Model. *Cancer Res.* **2001**, *61*, 7518–7524.
- Brockmann, M. A.; Papadimitriou, A.; Brandt, M.; Fillbrandt, R.; Westphal, M.; Lamszus, K. Inhibition of Intracerebral Glioblastoma Growth by Local Treatment with the Scatter Factor/Hepatocyte Growth Factor-Antagonist NK4. *Clin. Cancer Res.* **2003**, *9*, 4578–4585.
- Michieli, P.; Mazzone, M.; Basilico, C.; Cavassa, S.; Sottile, A.; Naldini, L.; Comoglio, P. M. Targeting the Tumor and its Microenvironment by a Dual-Function Decoy Met Receptor. *Cancer Cell* **2004**, *6*, 61–73.
- Kong-Beltran, M.; Stamos, J.; Wickramasinghe, D. The Sema Domain of Met Is Necessary for Receptor Dimerization and Activation. *Cancer Cell* **2004**, *6*, 75–84.
- Abounader, R.; Ranganathan, S.; Lal, B.; Fielding, K.; Book, A.; Dietz, H.; Burger, P.; Laterra, J. Reversion of Human Glioblastoma Malignancy by U1 Small Nuclear RNA/Ribozyme Targeting of Scatter Factor/Hepatocyte Growth Factor and c-Met Expression. *J. Natl. Cancer. Inst.* **1999**, *91*, 1548–1556.
- Kim, S. J.; Johnson, M.; Koterba, K.; Herynk, M. H.; Uehara, H.; Gallick, G. E. Reduced c-Met Expression by an Adenovirus Expressing a c-Met Ribozyme Inhibits Tumorigenic Growth and Lymph Node Metastases of PC3-LN4 Prostate Tumor Cells in an Orthotopic Nude Mouse Model. *Clin. Cancer Res.* **2003**, *9*, 5161–5170.
- Sattler, M.; Pride, Y. B.; Ma, P.; Gramlich, J. L.; Chu, S. C.; Quinlan, L. A.; Shirazian, S.; Liang, C.; Podar, K.; Christensen, J. G.; Salgia, R. A Novel Small Molecule Met Inhibitor Induces Apoptosis in Cells Transformed by the Oncogenic TPR-MET Tyrosine Kinase. *Cancer Res.* **2003**, *63*, 5462–5469.
- Wang, X.; Le, P.; Liang, C.; Chan, J.; Kiewlich, D.; Miller, T.; Harris, D.; Sun, L.; Rice, A.; Vasile, S.; Blake, R. A.; Howlett, A. R.; Patel, N.; McMahon, G.; Lipson, K. E. Potent and Selective Inhibitors of the Met [Hepatocyte Growth Factor/Scatter Factor (HGF/SF) Receptor] Tyrosine Kinase Block HGF/SF-Induced Tumor Cell Growth and Invasion. *Mol. Cancer Ther.* **2003**, *2*, 1085–1092.
- Christensen, J. G.; Schreck, R.; Burrows, J.; Kuruganti, P.; Chan, E.; Le, P.; Chen, J.; Wang, X.; Ruslim, L.; Blake, R.; Lipson, K. E.; Ramphal, J.; Do, S.; Cui, J. J.; Cherrington, J. M.; Mendel, D. B. A Selective Small Molecule Inhibitor of c-Met Kinase Inhibits c-Met-Dependent Phenotypes In Vitro and Exhibits Cytoreductive Antitumor Activity In Vivo. *Cancer Res.* **2003**, *63*, 7345–7355.
- Cui, J. J. Inhibitors Targeting Hepatocyte Growth Factor Receptor and their Potential Therapeutic Applications. *Expert Opin. Ther. Pat.* **2007**, *17*, 1035–1045.
- Zou, H. Y.; Li, Q.; Lee, J. H.; Arango, M. E.; McDonnell, S. R.; Yamazaki, S.; Koudriakova, T. B.; Alton, G.; Cui, J. J.; Kung, P. P.; Nambu, M. D.; Los, G.; Bender, S. L.; Mroczkowski, B.; Christensen, J. G. An Orally Available Small-Molecule Inhibitor of c-Met, PF-2341066, Exhibits Cytoreductive Antitumor Efficacy through Antiproliferative and Antiangiogenic Mechanisms. *Cancer Res.* **2007**, *67*, 4408–4417.
- Bellon, S. F.; Kaplan-Lefko, P.; Yang, Y.; Zhang, Y.; Moriguchi, J.; Rex, K.; Johnson, C. W.; Rose, P. E.; Long, A. M.; O'Connor, A. B.; Gu, Y.; Coxon, A.; Kim, T. S.; Tasker, A.; Burgess, T. L.; Dussault, I. c-Met Inhibitors with Novel Binding Mode Show Activity against Several Hereditary Papillary Renal Cell Carcinoma-Related Mutations. *J. Biol. Chem.* **2008**, *283*, 2675–2683.
- Albrecht, B. K.; Harmange, J.-C.; Bauer, D.; Berry, L.; Bode, C.; Boezio, A. A.; Chen, A.; Choquette, D.; Dussault, I.; Fridrich, C.; Hirai, S.; Hoffman, D.; Larrow, J. F.; Kaplan-Lefko, P.; Lin, J.; Lohman, J.; Long, A. M.; Moriguchi, J.; O'Connor, A.; Potashman, M. H.; Reese, M.; Rex, K.; Siegmund, A.; Shah, K.; Shimanovich, R.; Springer, S. K.; Teffera, Y.; Yang, Y.; Zhang, Y.; Bellon, S. F. Discovery and Optimization of Triazolopyridazines as Potent and Selective Inhibitors of the c-Met Kinase. *J. Med. Chem.* **2008**, *51*, 2879–2882.
- Fujiwara, Y.; Senga, T.; Nishitoba, T.; Osawa, T.; Miwa, A.; Nakamura, K. Quinoline Derivative and Quinazoline Derivative Inhibiting Self-Phosphorylation of Hepatocytus Proliferator Receptor, and Medicinal Composition Containing the Same. PCT Int. Appl. WO03000660A1, 2003.
- Compound **4** exhibited a K_i of 219 nM against KDR, a K_i of 65 nM against RON, and a K_i of 211 nM against IGFR. Harmange, J. C.; Booker, S.; Bauer, D.; Kim, T. S.; Cheng, Y.; Xu, S.; Xi, N.; Kim, J. L.; Tasker, A. Preparation of Heteroarylloxy Substituted Quinolines for Treating or Preventing HGF Mediated Diseases. PCT Int. Appl. WO05073224A2, 2005.
- Spychala, J. A Facile Preparation of N2-Arylisocytosines. *Synth. Commun.* **1997**, *27*, 1943–1949.

- (32) Walker, S. D.; Barder, T. E.; Martilelli, J. R.; Buchwald, S. L. A Rationally Designed Universal Catalyst for Suzuki-Miyaura Coupling Processes. *Angew. Chem., Int. Ed.* **2004**, *43*, 1871–1876.
- (33) Angioletti, M. E.; Casalnuovo, A. L.; Selby, T. P. Palladium-Catalyzed Cross-Coupling of Benzylzinc Reagents with Methylthio N-Heterocycles: A New Coupling Reaction with Unusual Selectivity. *Synlett* **2000**, *6*, 905–907.
- (34) Thomas, A. P.; Hennequin, L. F. A.; Ple, P. A. Quinoline Derivatives Inhibiting the Effect of Growth Factors such as VEGF. PCT Int. Appl. WO9813350A1, 1998.
- (35) Ife, R. J.; Leach, C. A. Amidine Derivatives as Gastric Acid Secretion Inhibitors. PCT Int. Appl. WO9426715A1, 1994.
- (36) Brown, D. J.; Cronin, B. J.; Lan, S. B.; Nardo, G. Heterocyclic Amplifiers of Phleomycin. VII. Phenyl-, Toly-, Phenoxy- and Benzylpyrimidines: Also Some Carbocyclic Analogs. *Aust. J. Chem.* **1985**, *38*, 825–833.
- (37) Lokensgard, J. P.; Fischer, J. W.; Bartz, W. J. Synthesis of *N*-(α -Methoxyalkyl) Amides from Imidates. *J. Org. Chem.* **1985**, *50*, 5609–5611.
- (38) Suzuki, A. Recent Advances in the Cross-Coupling Reactions of Organoboron Derivatives with Organic Electrophiles, 1995–1998. *J. Organomet. Chem.* **1999**, *576*, 147–168, and references therein.
- (39) Negishi, E.; King, A. O.; Okukado, N. J. Selective Carbon–Carbon Bond Formation via Transition Metal Catalysis. 3. A Highly Selective Synthesis of Unsymmetrical Biaryls and Diarylmethanes by the Nickel- or Palladium-Catalyzed Reaction of Aryl- and Benzylzinc Derivatives with Aryl Halides. *J. Org. Chem.* **1977**, *42*, 1821–1823.
- (40) Potashman, M.; Kim, T. S.; Bellon, S.; Booker, S.; Cheng, Y.; Kim, J. L.; Tasker, A.; Xi, N.; Xu, S.; Harmange, J. C.; Borg, G.; Weiss, M.; Hodous, B. L.; Graceffa, R.; Buckner, W. H.; Masse, C. E.; Choquette, D.; Martin, M. W.; Germain, J.; Dipietro, L. V.; Chaffee, S. C.; Nunes, J. J.; Buchanan, J. L.; Habgood, G. J.; McGowan, D. C.; Whittington, D. A. Preparation of Heteroaryl Substituted Naphthalenes as Inhibitors of Lck, VEGFR, and/or HGF Related Activity. PCT Int. Appl. WO05070891A2, 2005.
- (41) Harmange, J. C.; Booker, S.; Bauer, D.; Kim, T. S.; Cheng, Y.; Xu, S.; Xi, N.; Kim, J. L.; Tasker, A. Preparation of Heteroaryl Substituted Quinolines for Treating or Preventing HGF Mediated Diseases. PCT Int. Appl. WO05073224A2, 2005.
- (42) A table of the studied kinases is presented in the Supporting Information.
- (43) Still, W. C.; Kahn, M.; Mitra, A. Rapid Chromatographic Technique for Preparative Separations with Moderate Resolution. *J. Org. Chem.* **1978**, *43*, 2923–2925.
- (44) Polverino, A.; Coxon, A.; Starnes, C.; Diaz, Z.; DeMelfi, T.; Wang, L.; Bready, J.; Estrada, J.; Cattley, R.; Kaufman, S.; Chen, D.; Gan, Y.; Kumar, G.; Meyer, J.; Neervannan, S.; Alva, G.; Talvenheimo, J.; Montestruque, S.; Tasker, A.; Patel, V.; Radinsky, R.; Kendall, R. AMG 706, an Oral, Multikinase Inhibitor that Selectively Targets Vascular Endothelial Growth Factor, Platelet-Derived Growth Factor, and Kit Receptors, Potently Inhibits Angiogenesis and Induces Regression in Tumor Xenografts. *Cancer Res.* **2006**, *66*, 8715–8721.

JM8006189